Shape diagrams for 2D compact sets - Part I: analytic convex sets. Australian Journal of

Séverine Rivollier, Johan Debayle, Jean-Charles Pinoli

SHAPE DIAGRAMS FOR 2D COMPACT SETS - PART I: ANALYTIC CONVEX SETS

S. RIVOLLIER, J. DEBAYLE AND J.-C. PINOLI

Abstract. Shape diagrams are representations in the Euclidean plane introduced to study 3-dimensional and 2-dimensional compact convex sets. Such a set is represented by a point within a shape diagram whose coordinates are morphometrical functionals defined as normalized ratios of geometrical functionals. Classically, the geometrical functionals are the area, the perimeter, the radii of the inscribed and circumscribed circles, and the minimum and maximum Feret diameters. They allow thirty-one shape diagrams to be built. Most of these shape diagrams can also been applied to more general compact sets than compact convex sets. Starting from these six classical geometrical functionals, a detailed comparative study has been performed in order to analyze the representation relevance and discrimination power of these thirty-one shape diagrams. The purpose of this paper is to present the first part of this study, by focusing on analytic compact convex sets. A set will be called analytic if its boundary is piecewise defined by explicit functions in such a way that the six geometrical functionals can be straightforwardly calculated. The second and third part of the comparative study are published in two following papers [19, 20]. They are focused on analytic simply connected sets and convexity discrimination for analytic and discretized simply connected sets, respectively.

1 Introduction

The Blaschke's shape diagram [1, 2] allows to represent a 3D compact convex set by a point in the Euclidean 2D plane from three geometrical functionals: the volume, the surface area and the integral of mean curvature. The axes of this shape diagram are defined from geometric inequalities relating these functionals. These geometric inequalities do not provide a complete system: for any range of numerical values satisfying them, a compact convex set with these values for the geometrical functionals does not necessarily exist (in other words, a point within the 2D Blaschke shape diagram does not necessarily describe a 3D compact convex set).

Following the approach of Blaschke, Santalo [21] considered the shape diagrams of 2D compact convex sets from six geometrical functionals: the area, the perimeter, the radii of the inscribed and circumscribed circles, and the minimum and maximum Feret diameters [8]. Several studies on these shape diagrams have been performed [5, 9, 10, 11, 12, 21], but they were mainly restricted to the complete systems of inequalities for some triplets of these geometrical functionals.

This paper focuses on the study of shape diagrams for a wide range of 2D non-empty analytic compact convex sets. This study is not limited to complete systems of inequalities. The considered compact convex sets are mapped onto points in these shape diagrams, and through dispersion and overlapping quantifications, the shape

Key words and phrases. Analytic compact convex sets, Geometrical and morphometrical functionals, Shape diagrams, Shape discrimination.

diagrams are classified according to their ability to discriminate the compact convex sets.

2 Shape functionals

In this paper, the non-empty analytic compact convex sets in the Euclidean 2-space $\mathbb{E}^2$ are considered. A set will be called analytic if its boundary is piecewise defined by explicit functions in such a way that the geometrical functionals enumerated below can be calculated. These geometrical functionals are determinated in order to characterize the sets. They are related by the so-called geometric inequalities, which allow to define morphometrical functionals.

2.1 Geometrical functionals For a compact convex set in $\mathbb{E}^2$, let A, P, r, R, ω, d, denote its area, its perimeter, the radii of its inscribed and circumscribed circles, its minimum and maximum Feret diameters [8], respectively. Figure 2.1 illustrates some of these geometrical functionals.

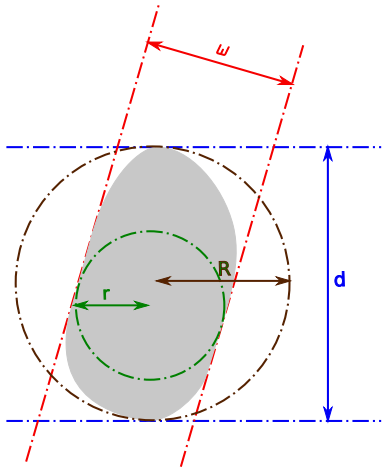

*Figure 2.1: Geometrical functionals of a compact convex set: radii of inscribed (*r*) and circumscribed (*R*) circles, minimum (ω) and maximum (*d*) Feret diameters.*

For a compact convex set, these six geometrical functionals are greater than zero. The line segments provide null values for A, r and ω, and the points for P, R and d.

2.2 Geometric inequalities For a compact convex set in $\mathbb{E}^2$, the relationships between these geometrical functionals are constrained by the geometric inequalities [4, 13, 14, 15, 22, 23, 24, 26] referenced in the second column of Table 2.1. These inequalities link geometrical functionals by pairs and determine the so-called extremal compact convex sets that satisfy the corresponding equalities (Table 2.1, fourth column). Futhermore, they allow to determinate morphometrical functionals.

2.3 Morphometrical functionals The morphometrical functionals are invariant under similitude transformations (consequently, they do not depend on the global size of the compact convex set) and are defined as ratios between geometrical functionals. In these ratios, the units of the numerator and the denominator are dimensionally homogeneous and the result has therefore no unit. Moreover, a normalization by a constant value (scalar multiplication) allows to have a ratio that

ranges in $[0, 1]$. For each morphometrical functional, the scalar value depends directly on the associated geometric inequality. These morphometrical functionals are referenced in the third column of Table 2.1.

These morphometrical functionals are classified according to their concrete meanings namely:

- roundness: $4\pi\,\mathrm{A}\,/\,\mathrm{P}^2$, $4\,\mathrm{A}\,/\pi\,\mathrm{d}^2$, $\pi\,\mathrm{r}^2\,/\,\mathrm{A}$ and $\mathrm{A}\,/\pi\,\mathrm{R}^2$;
- circularity: $2\pi\,\mathrm{r}\,/\,\mathrm{P}$, $\mathrm{P}\,/2\pi\,\mathrm{R}$, $\mathrm{r}\,/\,\mathrm{R}$, $2\,\mathrm{r}\,/\,\mathrm{d}$ and $\omega\,/2\,\mathrm{R}$;
- diameter constancy: $\pi\,\omega\,/\,\mathrm{P}$, $\mathrm{P}\,/\pi\,\mathrm{d}$ and $\omega\,/\,\mathrm{d}$;
- thinness: $2\,\mathrm{d}\,/\,\mathrm{P}$ and $4\,\mathrm{R}\,/\,\mathrm{P}$;
- equilateral triangularity: $\omega\,/3\,\mathrm{r}$ and $\omega^2\,/\sqrt{3}\,\mathrm{A}$.

The morphometrical functional $\sqrt{3}\,\mathrm{R}\,/\,\mathrm{d}$ expresses both the equilateral triangularity and the diameter constancy. The ratios $2\,\mathrm{r}\,/\,\omega$ and $\mathrm{d}\,/2\,\mathrm{R}$ do not have concrete meaning, they are equal to one for some different compact convex sets.

For example, the morphometrical functionals values are represented in Figure 2.2 for some 2D elementary analytic compact convex sets represented in Figure 2.3. These elementary compact convex sets constitute the family $\mathcal{F}_1^c$:

- line segments;
- equilateral triangles;
- Reuleaux triangles [7, 18]: curves of constant diameter constructed by taking the three points at the corners of an equilateral triangle and connecting each pair of points by a circular arc centered at the remaining point;
- squares;
- "Reuleaux" squares: curves by taking the four edge middles of a square and connecting each pair of opposite points by a circular arc centered at the remaining edge middle;
- disks;
- semi-disks;
- isosceles rectangle triangles;
- "1/2" diamonds: diamonds with $\pi/3$ and $\pi/6$ angles;
- "1/2" rectangles: rectangles with length/width=1/2;
- "1/2" ellipses: ellipses with major axis length/minor axis length=1/2;
- regular pentagons;
- regular hexagons.

For instance, let be a Reuleaux triangle constructed from an equilateral triangle of edge length denoted l. The Reuleaux triangle has a constant Feret diameter: $\mathrm{d} = \omega$. Futhermore,

$$\omega = l, \quad \mathrm{d} = l, \quad \mathrm{r} = l\left(1 - \frac{1}{\sqrt{3}}\right), \quad \mathrm{R} = \frac{l}{\sqrt{3}}, \quad \mathrm{P} = \pi l, \quad \mathrm{A} = l^2\left(\frac{\pi - \sqrt{3}}{2}\right).$$

All these geometrical functionals are expressed in function of l, term which disappears in the computation of the morphometrical functionals. For example,

$$\frac{\mathrm{A}}{\pi\,\mathrm{R}^2} = 3\left(\frac{\pi - \sqrt{3}}{2\pi}\right), \qquad \frac{\mathrm{P}}{\pi\,\mathrm{d}} = 1, \qquad \frac{2\,\mathrm{d}}{\mathrm{P}} = 2/\pi, \qquad \frac{\omega^2}{\sqrt{3}\,\mathrm{A}} = \frac{2}{\sqrt{3}(\pi - \sqrt{3})}.$$

The line segments are particular compact convex sets in the sense that some morphometrical functionals are zero-valued and some other ones are undefined because

A, r, ω are equal to zero. Figure 2.2 does not differenciate the roundness of the line segments which is null, and their equilateral triangularity which is undefined.

Table 2.1 synthesizes the geometrical and morphometrical functionals, the geometric inequalities and the extremal 2D analytic compact convex sets.

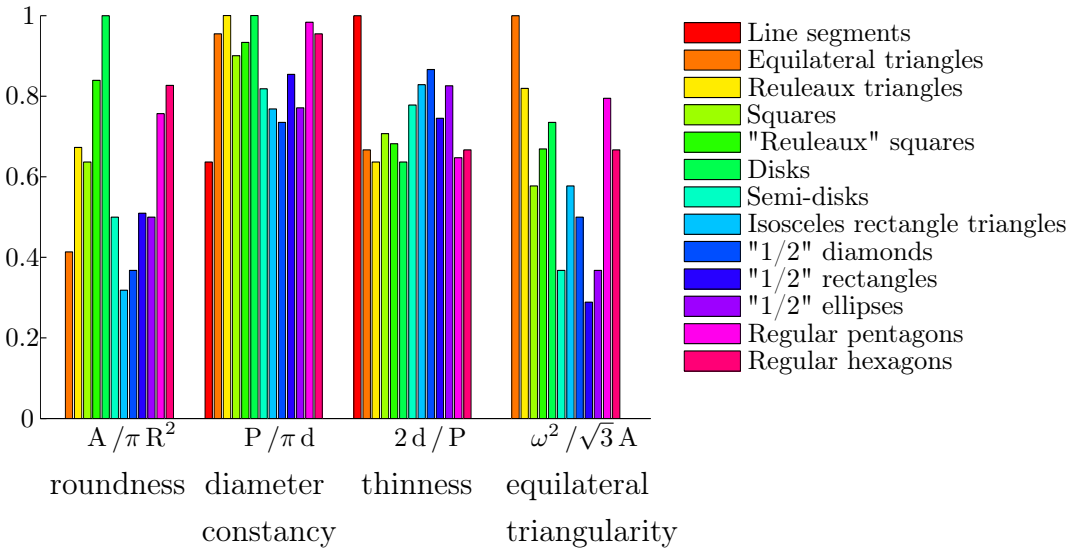

Figure 2.2: Values of several morphometrical functionals for elementary 2D compact convex sets.

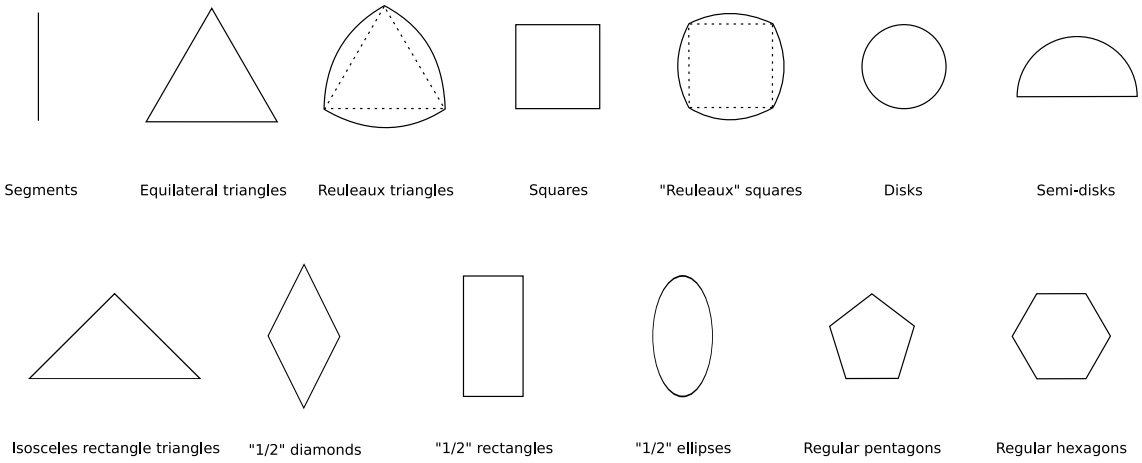

Figure 2.3: Family $\mathcal{F}_1^c$ of 2D analytic compact convex sets.

Geometrical functionals	**Geometric inequalities**	**Morphometrical functionals**	**Extremal sets**
r, R	$\mathrm{r} \leq \mathrm{R}$	r / R	C
ω, R	$\omega \leq 2\,\mathrm{R}$	$\omega / 2\,\mathrm{R}$	C
A, R	$\mathrm{A} \leq \pi\,\mathrm{R}^2$	$\mathrm{A} / \pi\,\mathrm{R}^2$	C
P, R	$\mathrm{P} \leq 2\pi\,\mathrm{R}$	$\mathrm{P} / 2\pi\,\mathrm{R}$	C
d, R	$\mathrm{d} \leq 2\,\mathrm{R}$	$\mathrm{d} / 2\,\mathrm{R}$	X
r, d	$2\,\mathrm{r} \leq \mathrm{d}$	$2\,\mathrm{r} / \mathrm{d}$	C
ω, d	$\omega \leq \mathrm{d}$	ω / d	W
A, d	$4\,\mathrm{A} \leq \pi\,\mathrm{d}^2$	$4\,\mathrm{A} / \pi\,\mathrm{d}^2$	C
P, d	$\mathrm{P} \leq \pi\,\mathrm{d}$	$\mathrm{P} / \pi\,\mathrm{d}$	W
R, d	$\sqrt{3}\,\mathrm{R} \leq \mathrm{d}$	$\sqrt{3}\,\mathrm{R} / \mathrm{d}$	Z
r, P	$2\pi\,\mathrm{r} \leq \mathrm{P}$	$2\pi\,\mathrm{r} / \mathrm{P}$	C
ω, P	$\pi\,\omega \leq \mathrm{P}$	$\pi\,\omega / \mathrm{P}$	W
A, P	$4\pi\,\mathrm{A} \leq \mathrm{P}^2$	$4\pi\,\mathrm{A} / \mathrm{P}^2$	C
d, P	$2\,\mathrm{d} \leq \mathrm{P}$	$2\,\mathrm{d} / \mathrm{P}$	L
R, P	$4\,\mathrm{R} \leq \mathrm{P}$	$4\,\mathrm{R} / \mathrm{P}$	L
r, A	$\pi\,\mathrm{r}^2 \leq \mathrm{A}$	$\pi\,\mathrm{r}^2 / \mathrm{A}$	C
ω, A	$\omega^2 \leq \sqrt{3}\,\mathrm{A}$	$\omega^2 / \sqrt{3}\,\mathrm{A}$	T
r, ω	$2\,\mathrm{r} \leq \omega$	$2\,\mathrm{r} / \omega$	X
ω, r	$\omega \leq 3\,\mathrm{r}$	$\omega / 3\,\mathrm{r}$	T

Extremal sets are the sets for which an inequality becomes an equality.
C the disks
T the equilateral triangles
W the constant width compact convex sets
L the line segments
X some compact convex sets
Z every compact convex set of diameter d containing an equilateral triangle of side-length d

Table 2.1: Shape functionals for compact convex sets. A, P, r, R, ω, d, *denote the area, perimeter, radii of the inscribed and circumscribed circles, minimum and maximum Feret diameters [8], respectively.*

3 Shape diagrams

From these morphometrical functionals, 2D shape diagrams can be defined. They enable to represent the morphology of any analytic compact convex sets in the Euclidean 2D plane from two morphometrical functionals (that is to say from three geometrical functionals because the two denominators use the same geometrical functionals).

3.1 Definition Let be any triplet of the considered six geometrical functionals (A, P, r, R, ω, d) and (M_1, M_2) be some particular morphometrical functionals valued in $[0,1]^2$ (Table 3.1). A shape diagram $\mathcal{D}$ is represented in the plane domain $[0,1]^2$ (whose axis coordinates are the morphometrical functionals M_1 and M_2) where any 2D compact set S is mapped onto a point (x, y). Note that if M_1 or M_2 is in

$\{\omega\,/\sqrt{3}\,\mathrm{A}, \pi\,\mathrm{r}^2\,/\,\mathrm{A}, 2\,\mathrm{r}\,/\,\omega, \omega\,/3\,\mathrm{r}\}$, the line segments can not be mapped onto a point because they provide null values for A, r and ω. In other terms, a shape diagram $\mathcal{D}$ is obtained from the following mapping:

$$\mathcal{D} : \left\{ \begin{array}{ccc} \mathcal{K}(\mathbb{E}^2) & \rightarrow & [0,1]^2 \\ S & \mapsto & (x,y) \end{array} \right.$$

where $\mathcal{K}(\mathbb{E}^2)$ denotes the compact sets of the Euclidean 2D plane. Using the morphometrical functionals listed in Table 2.1, thirty-one shape diagrams are defined, denoted $(\mathcal{D}_k)_{k\in[\![1,31]\!]}$, respectively.

Shape diagrams	**Axes coordinates**	
$\mathcal{D}_1 : (\omega, \mathrm{r}, \mathrm{R})$	$x = \omega\,/2\,\mathrm{R}$	$y = \mathrm{r}\,/\,\mathrm{R}$
$\mathcal{D}_2 : (\omega, \mathrm{A}, \mathrm{R})$	$x = \omega\,/2\,\mathrm{R}$	$y = \mathrm{A}\,/\pi\,\mathrm{R}^2$
$\mathcal{D}_3 : (\mathrm{r}, \mathrm{A}, \mathrm{R})$	$x = \mathrm{r}\,/\,\mathrm{R}$	$y = \mathrm{A}\,/\pi\,\mathrm{R}^2$
$\mathcal{D}_4 : (\mathrm{A}, \mathrm{d}, \mathrm{R})$	$x = \mathrm{A}\,/\pi\,\mathrm{R}^2$	$y = \mathrm{d}\,/2\,\mathrm{R}$
$\mathcal{D}_5 : (\omega, \mathrm{d}, \mathrm{R})$	$x = \omega\,/2\,\mathrm{R}$	$y = \mathrm{d}\,/2\,\mathrm{R}$
$\mathcal{D}_6 : (\mathrm{r}, \mathrm{d}, \mathrm{R})$	$x = \mathrm{r}\,/\,\mathrm{R}$	$y = \mathrm{d}\,/2\,\mathrm{R}$
$\mathcal{D}_7 : (\mathrm{A}, \mathrm{P}, \mathrm{R})$	$x = \mathrm{A}\,/\pi\,\mathrm{R}^2$	$y = \mathrm{P}\,/2\pi\,\mathrm{R}$
$\mathcal{D}_8 : (\omega, \mathrm{P}, \mathrm{R})$	$x = \omega\,/2\,\mathrm{R}$	$y = \mathrm{P}\,/2\pi\,\mathrm{R}$
$\mathcal{D}_9 : (\mathrm{r}, \mathrm{P}, \mathrm{R})$	$x = \mathrm{r}\,/\,\mathrm{R}$	$y = \mathrm{P}\,/2\pi\,\mathrm{R}$
$\mathcal{D}_{10} : (\mathrm{P}, \mathrm{d}, \mathrm{R})$	$x = \mathrm{P}\,/2\pi\,\mathrm{R}$	$y = \mathrm{d}\,/2\,\mathrm{R}$
$\mathcal{D}_{11} : (\omega, \mathrm{r}, \mathrm{d})$	$x = \omega\,/\,\mathrm{d}$	$y = 2\,\mathrm{r}\,/\,\mathrm{d}$
$\mathcal{D}_{12} : (\omega, \mathrm{A}, \mathrm{d})$	$x = \omega\,/\,\mathrm{d}$	$y = 4\,\mathrm{A}\,/\pi\,\mathrm{d}^2$
$\mathcal{D}_{13} : (\mathrm{r}, \mathrm{A}, \mathrm{d})$	$x = 2\,\mathrm{r}\,/\,\mathrm{d}$	$y = 4\,\mathrm{A}\,/\pi\,\mathrm{d}^2$
$\mathcal{D}_{14} : (\mathrm{A}, \mathrm{R}, \mathrm{d})$	$x = 4\,\mathrm{A}\,/\pi\,\mathrm{d}^2$	$y = \sqrt{3}\,\mathrm{R}\,/\,\mathrm{d}$
$\mathcal{D}_{15} : (\omega, \mathrm{R}, \mathrm{d})$	$x = \omega\,/\,\mathrm{d}$	$y = \sqrt{3}\,\mathrm{R}\,/\,\mathrm{d}$
$\mathcal{D}_{16} : (\mathrm{r}, \mathrm{R}, \mathrm{d})$	$x = 2\,\mathrm{r}\,/\,\mathrm{d}$	$y = \sqrt{3}\,\mathrm{R}\,/\,\mathrm{d}$
$\mathcal{D}_{17} : (\mathrm{A}, \mathrm{P}, \mathrm{d})$	$x = 4\,\mathrm{A}\,/\pi\,\mathrm{d}^2$	$y = \mathrm{P}\,/\pi\,\mathrm{d}$
$\mathcal{D}_{18} : (\omega, \mathrm{P}, \mathrm{d})$	$x = \omega\,/\,\mathrm{d}$	$y = \mathrm{P}\,/\pi\,\mathrm{d}$
$\mathcal{D}_{19} : (\mathrm{r}, \mathrm{P}, \mathrm{d})$	$x = 2\,\mathrm{r}\,/\,\mathrm{d}$	$y = \mathrm{P}\,/\pi\,\mathrm{d}$
$\mathcal{D}_{20} : (\mathrm{P}, \mathrm{R}, \mathrm{d})$	$x = \mathrm{P}\,/\pi\,\mathrm{d}$	$y = \sqrt{3}\,\mathrm{R}\,/\,\mathrm{d}$
$\mathcal{D}_{21} : (\omega, \mathrm{r}, \mathrm{P})$	$x = \pi\,\omega\,/\,\mathrm{P}$	$y = 2\pi\,\mathrm{r}\,/\,\mathrm{P}$
$\mathcal{D}_{22} : (\omega, \mathrm{A}, \mathrm{P})$	$x = \pi\,\omega\,/\,\mathrm{P}$	$y = 4\pi\,\mathrm{A}\,/\,\mathrm{P}^2$
$\mathcal{D}_{23} : (\mathrm{r}, \mathrm{A}, \mathrm{P})$	$x = 2\pi\,\mathrm{r}\,/\,\mathrm{P}$	$y = 4\pi\,\mathrm{A}\,/\,\mathrm{P}^2$
$\mathcal{D}_{24} : (\mathrm{A}, \mathrm{R}, \mathrm{P})$	$x = 4\pi\,\mathrm{A}\,/\,\mathrm{P}^2$	$y = 4\,\mathrm{R}\,/\,\mathrm{P}$
$\mathcal{D}_{25} : (\omega, \mathrm{R}, \mathrm{P})$	$x = \pi\,\omega\,/\,\mathrm{P}$	$y = 4\,\mathrm{R}\,/\,\mathrm{P}$
$\mathcal{D}_{26} : (\mathrm{r}, \mathrm{R}, \mathrm{P})$	$x = 2\pi\,\mathrm{r}\,/\,\mathrm{P}$	$y = 4\,\mathrm{R}\,/\,\mathrm{P}$
$\mathcal{D}_{27} : (\mathrm{A}, \mathrm{d}, \mathrm{P})$	$x = 4\pi\,\mathrm{A}\,/\,\mathrm{P}^2$	$y = 2\,\mathrm{d}\,/\,\mathrm{P}$
$\mathcal{D}_{28} : (\omega, \mathrm{d}, \mathrm{P})$	$x = \pi\,\omega\,/\,\mathrm{P}$	$y = 2\,\mathrm{d}\,/\,\mathrm{P}$
$\mathcal{D}_{29} : (\mathrm{r}, \mathrm{d}, \mathrm{P})$	$x = 2\pi\,\mathrm{r}\,/\,\mathrm{P}$	$y = 2\,\mathrm{d}\,/\,\mathrm{P}$
$\mathcal{D}_{30} : (\mathrm{d}, \mathrm{R}, \mathrm{P})$	$x = 2\,\mathrm{d}\,/\,\mathrm{P}$	$y = 4\,\mathrm{R}\,/\,\mathrm{P}$
$\mathcal{D}_{31} : (\omega, \mathrm{r}, \mathrm{A})$	$x = \omega^2\,/\sqrt{3}\,\mathrm{A}$	$y = \pi\,\mathrm{r}^2\,/\,\mathrm{A}$

Table 3.1: Axes coordinates of the thirty-one shape diagrams for 2D compact convex sets.

Property: The mapping which associates a 2D analytic compact convex set in $\mathbb{E}^2$ to a point in a shape diagram $(\mathcal{D}_k)_{k\in[\![1,31]\!]}$ is neither injective neither surjective.

Proof:

Non-injectivity: in each shape diagram, there exists points on which several 2D compact convex sets are mapped.

- Let be an ellipse with major and minor axes of length equal to 2 and 1 respectively, and a semi-disk of radius value equal to 1. These two sets have five similar geometrical functionals values: $\mathrm{A} = \pi/2$, $\omega = 1$, $\mathrm{d} = 2$, $\mathrm{r} = 0.5$, $\mathrm{R} = 1$. Thus, this ellipse and the semi-disk are mapped onto the same point in the shape diagrams $\mathcal{D}_1$, $\mathcal{D}_2$, $\mathcal{D}_3$, $\mathcal{D}_4$, $\mathcal{D}_5$, $\mathcal{D}_6$, $\mathcal{D}_{11}$, $\mathcal{D}_{12}$, $\mathcal{D}_{13}$, $\mathcal{D}_{14}$, $\mathcal{D}_{15}$, $\mathcal{D}_{16}$, $\mathcal{D}_{31}$.
- The diamond and ellipse perimeters are expressed in function of r and R by $4\sqrt{\mathrm{R}^2+\frac{\mathrm{r}^2\,\mathrm{R}^2}{\mathrm{R}^2-\mathrm{r}^2}}$ and $\pi\left(3(\mathrm{R}+\mathrm{r})-\sqrt{(\mathrm{R}+3\,\mathrm{r})(3\,\mathrm{R}+\mathrm{r})}\right)$ (Ramanujan), respectively. Notice that other approximations of the ellipse perimeter exist [17, 25]. When $\mathrm{R} = 1$, the equation

$$4\sqrt{\mathrm{R}^2+\frac{\mathrm{r}^2\,\mathrm{R}^2}{\mathrm{R}^2-\mathrm{r}^2}} = \pi\left(3(\mathrm{R}+\mathrm{r})-\sqrt{(\mathrm{R}+3\,\mathrm{r})(3\,\mathrm{R}+\mathrm{r})}\right)$$

  has a unique solution r in $\mathbb{R}_+$. Thus, an ellipse and a diamond with the same perimeter values, and the same inscribed and circumscribed radii values are found. Futhermore, for these two sets, $\omega = 2\,\mathrm{r}$ and $\mathrm{d} = 2\,\mathrm{R}$. Therefore, these two sets have five similar geometrical functionals values: R, d, r, ω, P. Consequently, this ellipse and this diamond are mapped onto the same point in the shape diagrams $\mathcal{D}_1$, $\mathcal{D}_5$, $\mathcal{D}_6$, $\mathcal{D}_8$, $\mathcal{D}_9$, $\mathcal{D}_{10}$, $\mathcal{D}_{11}$, $\mathcal{D}_{15}$, $\mathcal{D}_{16}$, $\mathcal{D}_{18}$, $\mathcal{D}_{19}$, $\mathcal{D}_{20}$, $\mathcal{D}_{21}$, $\mathcal{D}_{25}$, $\mathcal{D}_{26}$, $\mathcal{D}_{28}$, $\mathcal{D}_{29}$, $\mathcal{D}_{30}$.
- The diamond and ellipse areas are expressed in function of P and d by $\frac{\mathrm{d}^2\sqrt{\mathrm{P}^2-4\,\mathrm{d}^2}}{2\,\mathrm{P}}$ and $\frac{\mathrm{d}}{12}\left(3\,\mathrm{P}-2\pi\,\mathrm{d}-\sqrt{3\,\mathrm{P}^2+6\pi\,\mathrm{P}\,\mathrm{d}-5\pi^2\,\mathrm{d}^2}\right)$ (Ramanujan), respectively. When $\mathrm{d} = 2$, the equation

$$\frac{\mathrm{d}^2\sqrt{\mathrm{P}^2-4\,\mathrm{d}^2}}{2\,\mathrm{P}} = \frac{\mathrm{d}}{12}\left(3\,\mathrm{P}-2\pi\,\mathrm{d}-\sqrt{3\,\mathrm{P}^2+6\pi\,\mathrm{P}\,\mathrm{d}-5\pi^2\,\mathrm{d}^2}\right)$$

  has a unique solution P in $\mathbb{R}_+$. Thus, an ellipse and a diamond with the same area and perimeter values, and the same maximum Feret diameter values are found. Futhermore, for these two sets, $\mathrm{d} = 2\,\mathrm{R}$. Therefore, these two sets have four similar geometrical functionals values: R, d, P, A. Consequently, this ellipse and this diamond are mapped onto the same point in the shape diagrams $\mathcal{D}_4$, $\mathcal{D}_7$, $\mathcal{D}_{10}$, $\mathcal{D}_{14}$, $\mathcal{D}_{17}$, $\mathcal{D}_{20}$, $\mathcal{D}_{24}$, $\mathcal{D}_{27}$, $\mathcal{D}_{30}$.
- The rectangle and ellipse areas are expressed in function of P and ω by $\omega\,(\mathrm{P}/2-\omega)$ and $\frac{\omega}{12}\left(3\,\mathrm{P}-2\pi\,\omega+\sqrt{3\,\mathrm{P}^2+6\pi\,\mathrm{P}\,\omega-5\pi^2\,\omega^2}\right)$ (Ramanujan), respectively. When $\omega = 2$, the equation

$$\omega\,(\mathrm{P}/2-\omega) = \frac{\omega}{12}\left(3\,\mathrm{P}-2\pi\,\omega+\sqrt{3\,\mathrm{P}^2+6\pi\,\mathrm{P}\,\omega-5\pi^2\,\omega^2}\right)$$

has a unique solution P in $\mathbb{R}_+$. Thus, an ellipse and a rectangle with the same area and perimeter values, and the same minimum Feret diameter values are found. Futhermore, for these two sets, $\omega = 2\,\mathrm{r}$. Therefore, these two sets have four similar geometrical functionals values: r, ω, P, A. Consequently, this ellipse and this rectangle are mapped onto the same point in the shape diagrams $\mathcal{D}_{21}$, $\mathcal{D}_{22}$, $\mathcal{D}_{23}$, $\mathcal{D}_{31}$.

Non-surjectivity: in each shape diagram, there exists points on which none 2D compact convex set are mapped.

- $4\,\mathrm{R} \leq \mathrm{P}$ and $\mathrm{P} \leq 2\pi\,\mathrm{R}$ imply $\frac{2}{\pi} \leq \frac{4\,\mathrm{R}}{\mathrm{P}}$ and $\frac{2}{\pi} \leq \frac{\mathrm{P}}{2\pi\,\mathrm{R}}$.
  $2\,\mathrm{d} \leq \mathrm{P}$ and $\mathrm{P} \leq \pi\,\mathrm{d}$ imply $\frac{2}{\pi} \leq \frac{2\,\mathrm{d}}{\mathrm{P}}$ and $\frac{2}{\pi} \leq \frac{\mathrm{P}}{\pi\,\mathrm{d}}$.
  In the shape diagrams $\mathcal{D}_7$, $\mathcal{D}_8$, $\mathcal{D}_9$, $\mathcal{D}_{17}$, $\mathcal{D}_{18}$, $\mathcal{D}_{19}$, $\mathcal{D}_{24}$, $\mathcal{D}_{25}$, $\mathcal{D}_{26}$, $\mathcal{D}_{27}$, $\mathcal{D}_{28}$, $\mathcal{D}_{29}$, $\mathcal{D}_{30}$, on all points below the line of equation $y = 2/\pi$, none compact convex set are mapped.
  In the shape diagrams $\mathcal{D}_{10}$, $\mathcal{D}_{20}$, $\mathcal{D}_{30}$, on all points at the left of the line of equation $x = 2/\pi$, none compact convex set are mapped.
- $\sqrt{3}\,\mathrm{R} \leq \mathrm{d}$ and $\mathrm{d} \leq 2\,\mathrm{R}$ imply $\frac{\sqrt{3}}{2} \leq \frac{\sqrt{3}\,\mathrm{R}}{\mathrm{d}}$ and $\frac{\sqrt{3}}{2} \leq \frac{\mathrm{d}}{2\,\mathrm{R}}$.
  In the shape diagrams $\mathcal{D}_4$, $\mathcal{D}_5$, $\mathcal{D}_6$, $\mathcal{D}_{14}$, $\mathcal{D}_{15}$, $\mathcal{D}_{16}$, $\mathcal{D}_{10}$, $\mathcal{D}_{20}$, on all points below the line of equation $y = \sqrt{3}/2$, none compact convex set are mapped.
- $2\,\mathrm{r} \leq \omega$ implies $\frac{\mathrm{r}}{\mathrm{R}} \leq \frac{\omega}{2\,\mathrm{R}}$ and $\frac{2\,\mathrm{r}}{\mathrm{d}} \leq \frac{\omega}{\mathrm{d}}$ and $\frac{2\pi\,\mathrm{r}}{\mathrm{P}} \leq \frac{\pi\,\omega}{\mathrm{P}}$ and $\frac{\pi\,\mathrm{r}^2}{\mathrm{A}} \leq \frac{\pi\,\omega^2}{4\,\mathrm{A}}$.
  $\omega \leq 3\,\mathrm{r}$ implies $\frac{\omega}{2\,\mathrm{R}} \leq \frac{3\,\mathrm{r}}{2\,\mathrm{R}}$ and $\frac{\omega}{\mathrm{d}} \leq \frac{3\,\mathrm{r}}{\mathrm{d}}$ and $\frac{\pi\,\omega}{\mathrm{P}} \leq \frac{3\pi\,\mathrm{r}}{\mathrm{P}}$ and $\frac{\omega^2}{\sqrt{3}\,\mathrm{A}} \leq \frac{9\,\mathrm{r}^2}{\sqrt{3}\,\mathrm{A}}$.
  In the shape diagrams $\mathcal{D}_1$, $\mathcal{D}_{11}$, $\mathcal{D}_{21}$, on all points above the line of equation $y = x$ or below the line of equation $y = \frac{2}{3}x$, none compact convex set are mapped. In the shape diagram $\mathcal{D}_{31}$, on all points above the line of equation $y = \frac{\pi\sqrt{3}}{4}x$ or below the line of equation $y = \frac{\pi\sqrt{3}}{9}x$, none compact convex sest are mapped.
- $\omega^2 \leq \sqrt{3}\,\mathrm{A}$ implies $\left(\frac{\omega}{2\,\mathrm{R}}\right)^2 \leq \frac{\sqrt{3}\,\mathrm{A}}{4\,\mathrm{R}^2}$ and $\left(\frac{\omega}{\mathrm{d}}\right)^2 \leq \frac{\sqrt{3}\,\mathrm{A}}{\mathrm{d}^2}$ and $\left(\frac{\pi\,\omega}{\mathrm{P}}\right)^2 \leq \frac{\pi^2\sqrt{3}\,\mathrm{A}}{\mathrm{P}^2}$.
  In the shape diagrams $\mathcal{D}_2$, $\mathcal{D}_{12}$, $\mathcal{D}_{22}$, on all points below the line curve of equation $y = \frac{4}{\pi\sqrt{3}}x^2$, none compact convex set are mapped.
- $\pi\,\mathrm{r}^2 \leq \mathrm{A}$ implies $\left(\frac{\mathrm{r}}{\mathrm{R}}\right)^2 \leq \frac{\mathrm{A}}{\pi\,\mathrm{R}^2}$ and $\left(\frac{2\,\mathrm{r}}{\mathrm{d}}\right)^2 \leq \frac{4\,\mathrm{A}}{\pi\,\mathrm{d}^2}$ and $\left(\frac{2\pi\,\mathrm{r}}{\mathrm{P}}\right)^2 \leq \frac{4\pi\,\mathrm{A}}{\mathrm{P}^2}$.
  In the shape diagrams $\mathcal{D}_3$, $\mathcal{D}_{13}$, $\mathcal{D}_{23}$, on all points below the line curve of equation $y = x^2$, none compact convex set are mapped. □

3.2 Complete systems of inequalities A system of (two) geometric inequalities associated to a shape diagram is complete if and only if for any range of geometrical functionals values satisfying those conditions, a 2D compact convex set with these geometrical functionals values exists [10, 21]. In other words, such a system is complete if and only if the mapping which associates a 2D analytic compact convex set in $\mathbb{E}^2$ to a point in a shape diagram $(\mathcal{D}_k)_{k\in[\![1,31]\!]}$ can be surjective by restricting the arrival set. For a shape diagram, each of the two associated inequalities determines a part of the convex domain boundary (the domain in which all compact convex sets are mapped). These two inequalities determine the whole boundary of the convex domain if and only if they form a complete system. The compact convex sets mapped onto the boundary points are the extremal compact convex sets of each considered inequality.

For twenty-one among the thirty-one shape diagrams ($\mathcal{D}_1$, $\mathcal{D}_3$, $\mathcal{D}_4$, $\mathcal{D}_5$, $\mathcal{D}_6$, $\mathcal{D}_7$, $\mathcal{D}_9$, $\mathcal{D}_{10}$, $\mathcal{D}_{11}$, $\mathcal{D}_{12}$, $\mathcal{D}_{14}$, $\mathcal{D}_{15}$, $\mathcal{D}_{16}$, $\mathcal{D}_{18}$, $\mathcal{D}_{20}$, $\mathcal{D}_{22}$, $\mathcal{D}_{23}$, $\mathcal{D}_{24}$, $\mathcal{D}_{26}$, $\mathcal{D}_{28}$, $\mathcal{D}_{30}$), the completeness of systems of inequalities has been proved [5, 9, 10, 11, 12, 21]. Figure 4.1 illustrates the convex domain boundary for ten of them.

4 Shape diagrams dispersion quantification

4.1 Shape diagrams for compact convex sets For the family $\mathcal{F}_1^c$ of thirteen compact convex sets (Figure 2.3), the morphometrical functionals are straightforwardly computed. Each compact convex set $i \in [\![1, 13]\!]$ is represented by one point denoted $\mathcal{P}_{i,k}$, in each shape diagram $\mathcal{D}_k$, for $k \in [\![1, 31]\!]$.

Figure 4.2 illustrates several of these thirty-one shape diagrams, chosen according to the results synthetized in section 6. Remember that the shape diagrams are included in $[0, 1]^2$. For a better visualization of the shapes drawn on a point of abscissa or ordinate equal to 0 or 1, the shape diagrams are illustrated in $[-0.06, 1.04]^2$. Whatever the morphometrical functional, the extremal value 1 is reached for extremal compact convex sets. Thus, in each shape diagram, there is at least one compact convex set mapped to a point of abscissa or ordinate equal to 1. Moreover, the extremal value 0 is not always reached.

The dispersion of compact convex set locations within each shape diagram will be studied after the analysis of similarities between shape diagrams.

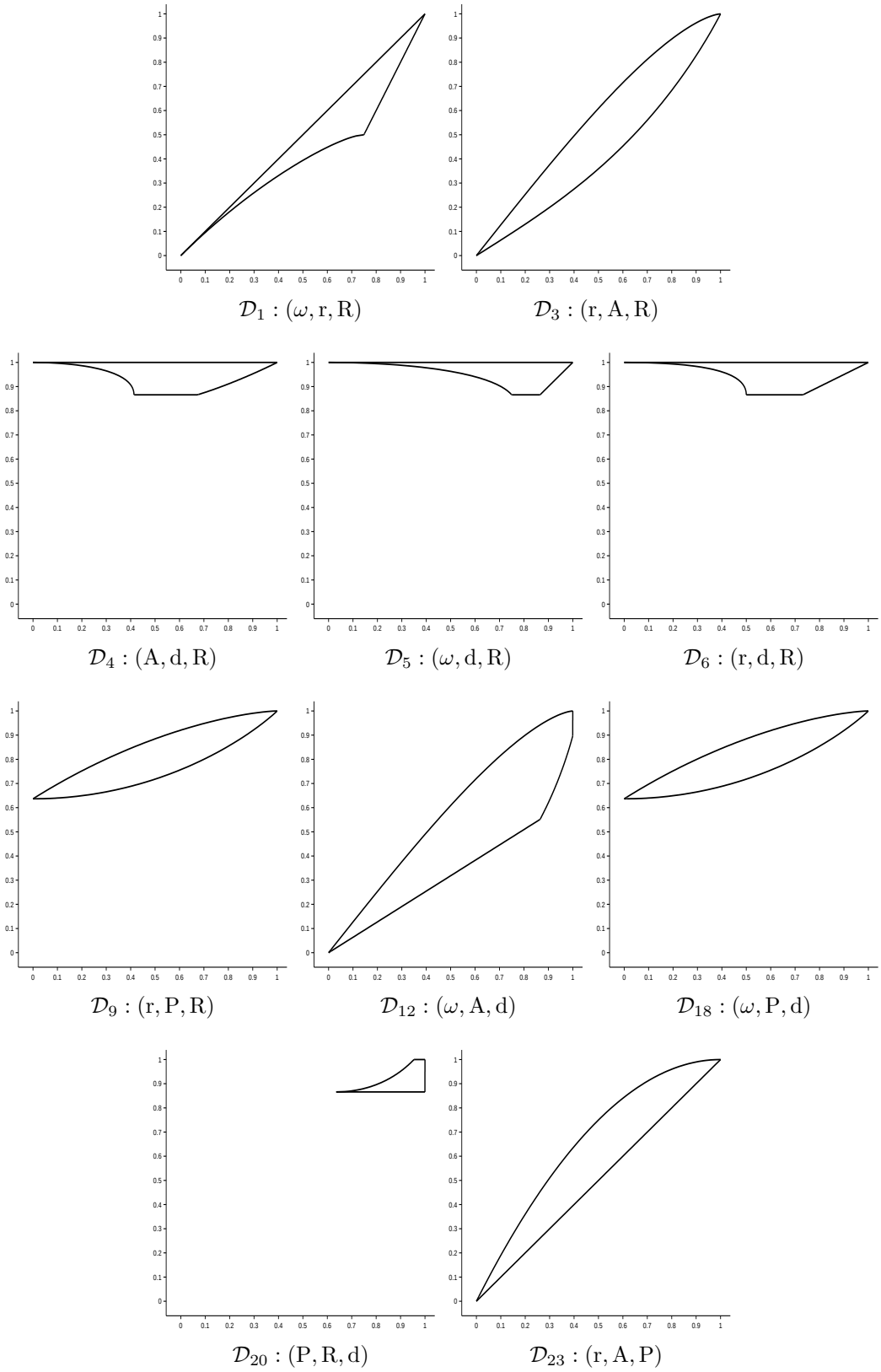

Figure 4.1: Convex domains of ten shape diagrams for which complete systems of inequalities have been established. For a given shape diagram, the bordered region represents the convex domain in which all compact convex sets lay.

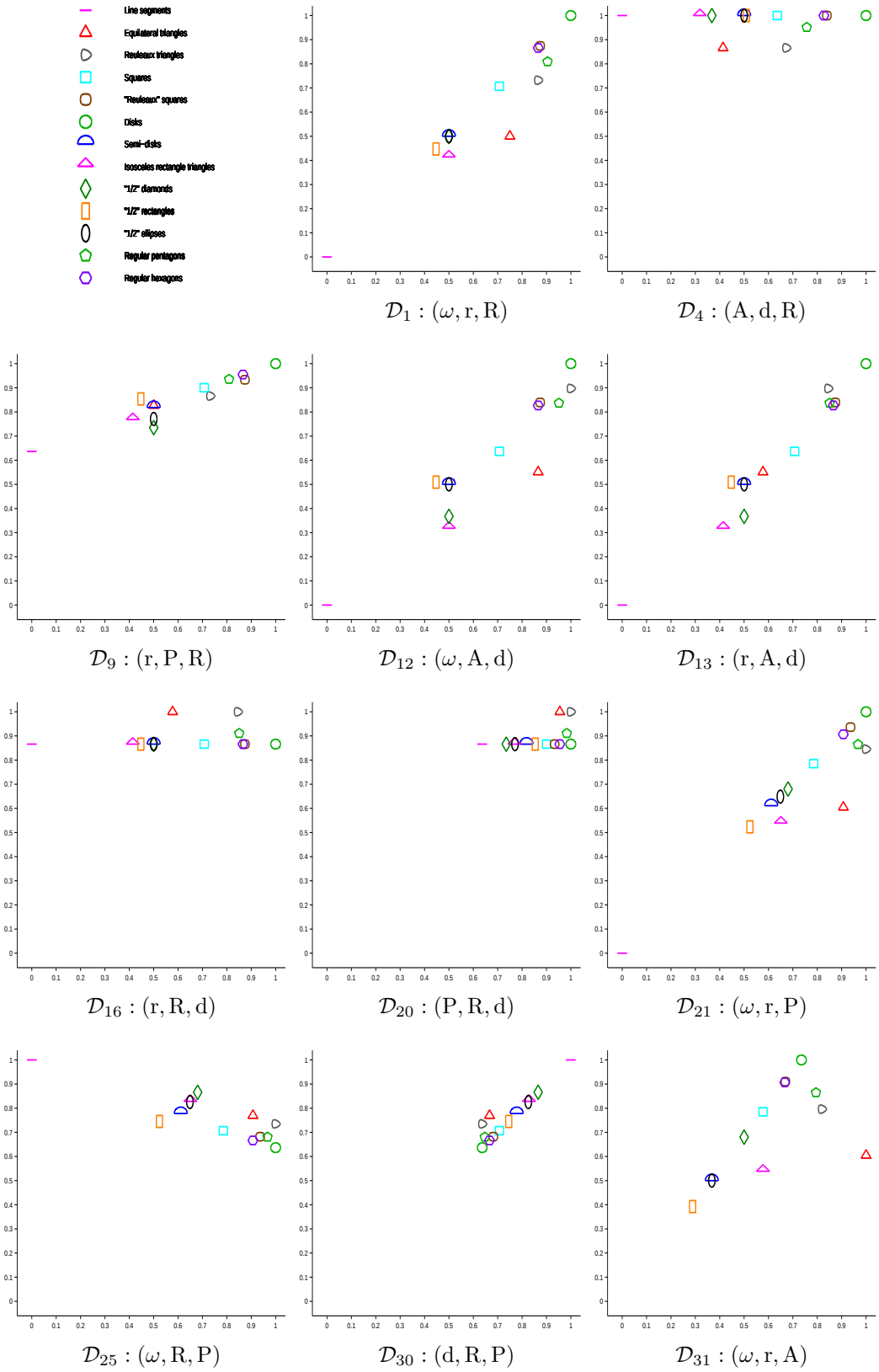

Figure 4.2: Family $\mathcal{F}_1^c$ of analytic compact convex sets mapped into eleven shape diagrams (chosen according to the results synthetized in section 6).

4.2 Similarity The fact that $\omega = 2\,\mathrm{r}$ for some compact convex sets implies that shape diagrams (ω, x_1, x_2) are similar to shape diagrams (r, x_1, x_2) where $x_1 \in \{\mathrm{d}, \mathrm{R}, \mathrm{P}, \mathrm{A}\}$ and $x_2 \in \{\mathrm{d}, \mathrm{R}, \mathrm{P}\}$, that is to say $\mathcal{D}_2 \sim \mathcal{D}_3$, $\mathcal{D}_5 \sim \mathcal{D}_6$, $\mathcal{D}_8 \sim \mathcal{D}_9$, $\mathcal{D}_{12} \sim \mathcal{D}_{13}$, $\mathcal{D}_{15} \sim \mathcal{D}_{16}$, $\mathcal{D}_{18} \sim \mathcal{D}_{19}$, $\mathcal{D}_{22} \sim \mathcal{D}_{23}$, $\mathcal{D}_{25} \sim \mathcal{D}_{26}$, $\mathcal{D}_{28} \sim \mathcal{D}_{29}$ where $\sim$ denotes a strong similarity between shape diagrams.

In the same way, the fact that $\mathrm{d} = 2\,\mathrm{R}$ for some compact convex sets implies that:

- shape diagrams (x_1, x_2, R) are similar to shape diagrams (x_1, x_2, d) where $x_1 \in \{\omega, \mathrm{r}, \mathrm{A}\}$ and $x_2 \in \{\mathrm{r}, \mathrm{A}, \mathrm{P}\}$ ($\mathcal{D}_1 \sim \mathcal{D}_{11}$, $\mathcal{D}_2 \sim \mathcal{D}_{12}$, $\mathcal{D}_3 \sim \mathcal{D}_{13}$, $\mathcal{D}_7 \sim \mathcal{D}_{17}$, $\mathcal{D}_8 \sim \mathcal{D}_{18}$, $\mathcal{D}_9 \sim \mathcal{D}_{19}$);
- shape diagrams $(x_1, \mathrm{R}, \mathrm{P})$ are similar to shape diagrams $(x_1, \mathrm{d}, \mathrm{P})$ where $x_1 \in \{\omega, \mathrm{r}, \mathrm{A}\}$ ($\mathcal{D}_{24} \sim \mathcal{D}_{27}$, $\mathcal{D}_{25} \sim \mathcal{D}_{28}$, $\mathcal{D}_{26} \sim \mathcal{D}_{29}$).

An algorithm of hierarchical classification [6] based on distances between shape diagrams allows to justify many of these similarities and to find other ones. Let $k_1, k_2 \in [\![1, 31]\!]$, the distance between shape diagrams $\mathcal{D}_{k_1}$ and $\mathcal{D}_{k_2}$, based on the Euclidean distance d^E, is defined by Equation 4.1.

$$d^E(\mathcal{D}_{k_1}, \mathcal{D}_{k_2}) = \frac{1}{13} \sum_{i \in [\![1,13]\!]} d^E\left(\mathcal{P}_{i,k_1}, \mathcal{P}_{i,k_2}\right) \tag{4.1}$$

For all $k_1 \in [\![1, 30]\!]$ and $k_2 \in [\![k_1 + 1, 31]\!]$, the distances $d^E(\mathcal{D}_{k_1}, \mathcal{D}_{k_2})$ are computed. Among them, the minimum distance value gives the best similarity between two shape diagrams. From these two shape diagrams, a mean shape diagram is built. To each step of the algorithm, two shape diagrams are similar up to the distance computed and they are gathered to build a mean shape diagram. The algorithm can be run until all the shape diagrams are gathered. Figure 4.3 shows the first twenty-three steps of the hierarchical tree resulting from this algorithm. The remaining steps are not shown because the distance values are too high and do not present an interest in the study of similarities.

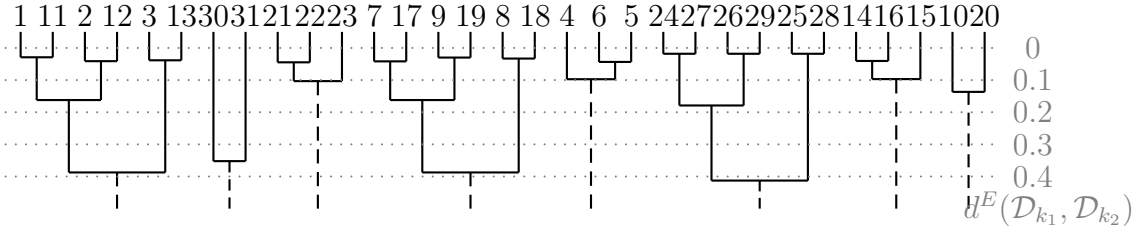

Figure 4.3: The first twenty-three steps of an algorithm of hierarchical classification based on distances between the shape diagrams. To each step, two shape diagrams are similar up to the distance value, whose the scale is indicated on the right.

For instance, if the algorithm is stopped before the distance value reaches 0.2, the following classification of shape diagrams is obtained:

- $\mathcal{D}_1$, $\mathcal{D}_{11}$, $\mathcal{D}_2$, $\mathcal{D}_{12}$
- $\mathcal{D}_7$, $\mathcal{D}_{17}$, $\mathcal{D}_9$, $\mathcal{D}_{19}$
- $\mathcal{D}_{24}$, $\mathcal{D}_{27}$, $\mathcal{D}_{26}\mathcal{D}_{29}$
- $\mathcal{D}_{10}$, $\mathcal{D}_{20}$
- $\mathcal{D}_{21}$, $\mathcal{D}_{22}$, $\mathcal{D}_{23}$
- $\mathcal{D}_4$, $\mathcal{D}_5$, $\mathcal{D}_6$
- $\mathcal{D}_{14}$, $\mathcal{D}_{15}$, $\mathcal{D}_{16}$
- $\mathcal{D}_{30}$
- $\mathcal{D}_3$, $\mathcal{D}_{13}$
- $\mathcal{D}_8$, $\mathcal{D}_{18}$
- $\mathcal{D}_{25}$, $\mathcal{D}_{28}$
- $\mathcal{D}_{31}$

4.3 Dispersion quantification For each shape diagram, the dispersion of the locations of 2D analytic compact convex sets of the family $\mathcal{F}_1^c$ is studied.

The spatial distribution of compact convex sets locations in each shape diagram is characterized and quantified from algorithmic geometry using Delaunay's graph (DG) and minimum spanning tree (MST) [3]. Some useful information about the disorder and the neighborhood relationships between sets can be deduced. From each geometrical model, it is possible to compute two values from the edge lengths, denoted μ (average) and σ (standard deviation) for DG or MST. The simple reading of the coordinates in the (μ, σ)-plane eanables to determine the type of spatial distribution of the compact convex set range (regular, random, cluster, ...) [16]. The decrease of μ and the increase of σ characterize the shift from a regular distribution toward random and cluster distributions, respectively.

Figure 4.4 represents both values of parameters of the thirty-one shape diagrams for each model, DG and MST.

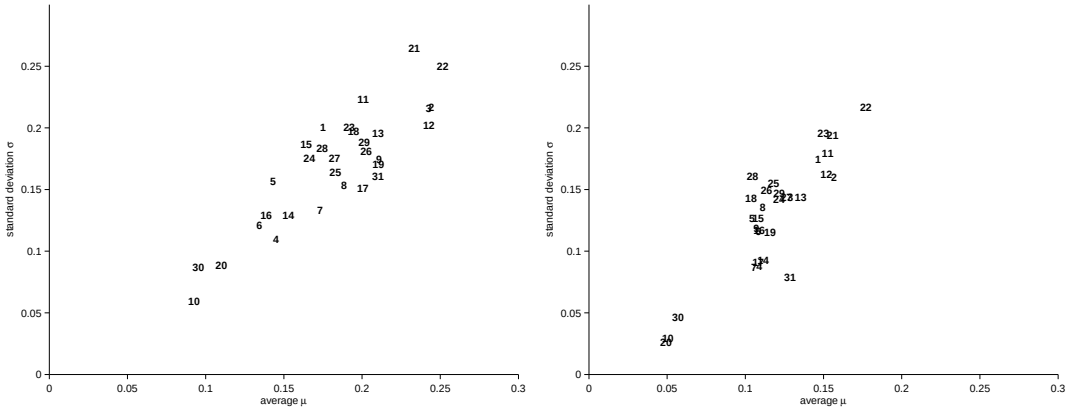

DG MST

Figure 4.4: Two dispersion quantifications for all shape diagrams applied on the family $\mathcal{F}_1^c$. For each representation (according to the models DG and MST, respectively), indices $k \in [\![1, 31]\!]$ of the shape diagrams $\mathcal{D}_k$ are located according to their μ and σ values.

MST enables to visually distinguish five groups of shape diagrams, according to their dispersion measurements (μ,σ):

- $\mathcal{D}_{22}$
- $\mathcal{D}_1$, $\mathcal{D}_{11}$, $\mathcal{D}_2$, $\mathcal{D}_{12}$, $\mathcal{D}_{21}$, $\mathcal{D}_{23}$
- $\mathcal{D}_{10}$, $\mathcal{D}_{20}$, $\mathcal{D}_{30}$
- $\mathcal{D}_4$, $\mathcal{D}_{14}$, $\mathcal{D}_7$, $\mathcal{D}_{17}$, $\mathcal{D}_{31}$
- the sixteen others.

DG also extracts the shape diagrams $\mathcal{D}_{10}$, $\mathcal{D}_{20}$, $\mathcal{D}_{30}$, that have both low μ and σ values. These three shape diagrams have a weak dispersion. Visually, the compact convex sets locations form a cluster (see Figure 4.2 for $\mathcal{D}_{20}$ and $\mathcal{D}_{30}$). The shape diagrams $\mathcal{D}_{21}$ and $\mathcal{D}_{22}$ have both high μ and σ values, that is to say a strong dispersion. Visually, the compact convex sets are located within a large domain within $[0, 1]^2$ and are well spaced from each other.

Finally, these statements are in agreement with those obtained for the similarities between shape diagrams.

A shape diagram with a strong dispersion (both high μ and σ values), for both DG and MST, guarantees a strong discrimination of shapes: the compact convex sets are located within a large domain in $[0,1]^2$ and are well spaced from each other. However, remember that $\mathrm{d} = 2\,\mathrm{R}$ and $\omega = 2\,\mathrm{r}$ for some compact convex sets. This explains that the compact convex sets of the family $\mathcal{F}_1^c$ - except for equilateral triangles, Reuleaux triangles, pentagons where $\mathrm{d} \neq 2\,\mathrm{R}$ and $\omega \neq 2\,\mathrm{r}$ and isosceles rectangle triangles where $\omega \neq 2\,\mathrm{r}$ - are mapped onto a point on a line for some shape diagrams, namely:

- diagonal line from $(0,0)$ to $(1,1)$ on shape diagrams (x_1, x_2, x_3) where $(x_1, x_2) \in \{(\omega, \mathrm{r}), (\mathrm{d}, \mathrm{R})\}$ and $x_3 \in \{\mathrm{A}, \mathrm{R}, \mathrm{d}, \mathrm{P}\}$ ($\mathcal{D}_1$, $\mathcal{D}_{11}$, $\mathcal{D}_{21}$, $\mathcal{D}_{30}$, $\mathcal{D}_{31}$)
- horizontal line from $(0,1)$ to $(1,1)$ on shape diagrams $(x_1, \mathrm{d}, \mathrm{R})$ where $x_1 \in \{\omega, \mathrm{r}, \mathrm{P}, \mathrm{A}\}$ ($\mathcal{D}_4$, $\mathcal{D}_5$, $\mathcal{D}_6$, $\mathcal{D}_{10}$)
- horizontal line from $(0, \sqrt{(}3)/2)$ to $(1, \sqrt{(}3)/2)$ on shape diagrams $(x_1, \mathrm{R}, \mathrm{d})$ where $x_1 \in \{\omega, \mathrm{r}, \mathrm{P}, \mathrm{A}\}$ ($\mathcal{D}_{14}$, $\mathcal{D}_{15}$, $\mathcal{D}_{16}$, $\mathcal{D}_{20}$)

For a shape diagram, the fact that some compact convex sets are mapped onto a point on a line does not yield to allow a strong discrimination of the compact convex sets as quantified and illustrated in Figure 4.4.

5 Shape diagrams overlapping quantification

5.1 Shape diagrams for compact convex sets with one degree of freedom

Let two 2D analytic compact convex sets of the family $\mathcal{F}_1^c$, and the compact convex set class allowing to switch from one to the other using one degree of freedom. For example, the line segment goes to the square through rectangles whose elongation decreases (or through diamonds, ...). Therefore, several classes of "compact convex sets with one degree of freedom" could be defined. Thus, a curve denoted $\mathcal{C}_{i,k}$ from each compact convex set class C_i is created in each shape diagram $\mathcal{D}_k$, $k \in [\![1, 31]\!]$. This process is used for some pairs of compact convex sets of the family $\mathcal{F}_1^c$. The tendency of various curves are observed.

These analytic compact convex sets verify shape properties which are preserved only under similitude transformations and under the variation of one parameter $t \in \mathbb{R}$. These are, for example, isosceles triangles (the "isosceles" property is preserved when the top angle varies between 0 and π), rectangles (the ratio width/length varies between 0 and 1), ... In other terms, the degree of freedom is the parameter $t \in \mathbb{R}$.

Twenty-three analytic compact convex set classes (chosen according to the faculty to compute analytically their geometrical (and morphometrical) functional values), gathered in four families, are considered:

- family $\mathcal{F}_{2.1}^c \supseteq \{C_i\}_{i \in [\![1,4]\!]}$: four classes of compact convex sets with one symmetrical axis (Figure 5.1),
- family $\mathcal{F}_{2.2}^c \supseteq \{C_i\}_{i \in [\![5,13]\!]}$: nine classes of compact convex sets with two symmetrical axes (Figure 5.2),
- family $\mathcal{F}_{2.3}^c \supseteq \{C_i\}_{i \in [\![14,18]\!]}$: five classes of compact convex sets with an odd number strictly greater to 1 of symmetrical axes (Figure 5.3),
- family $\mathcal{F}_{2.4}^c \supseteq \{C_i\}_{i \in [\![19,23]\!]}$: five classes of compact convex sets with an even number strictly greater to 2 of symmetrical axes (Figure 5.4).

There are:

- Family $\mathcal{F}^c_{2.1}$:
  C_1 - Isosceles triangles: The top angle varies in $[0, \pi]$. When it reaches the bounds, the isosceles triangle becomes a line segment.
  C_2 - Angular sectors: The angle varies in $[0, \pi]$. When it reaches the lower and upper bounds, the angular sector becomes a line segment and a semi-disk, respectively.
  C_3 - Ungula: They are based on angular sectors whose angle varies in $[0, \pi]$. The extremal compact convex sets are the point (null angle) and the semi-disk (angle equals to π).
  C_4 - Semi-symmetrical disks with two peaks: They are the convex hulls of a semi-disk and two symmetrically placed points. The disk radius value varies between 0 and the half of the line segment length. The extremal compact convex sets are the line segment and the semi-disk, respectively.
- Family $\mathcal{F}^c_{2.2}$:
  C_5 - Rectangles: The ratio between the width and the length varies in $[0, 1]$. When it reaches the lower and upper bounds, the rectangle becomes a line segment and a square, respectively.
  C_6 - Symmetrical disk segments: They are the intersection of a disk and a symmetrically placed strip. The extremal compact convex sets are the line segment and the disk.
  C_7 - Rectangles terminated by semi-disks: The ratio between the width and the length of the rectangle varies in $[0, 1]$. Semi-disks are placed on two opposite edges. When the ratio reaches the lower and upper bounds, the resulting compact convex set becomes a line segment and a disk, respectively.
  C_8 - Ellipses: The ratio between the minor and major axes lengths varies in $[0, 1]$. When it reaches the lower and upper bounds, the ellipse becomes a line segment and a disk, respectively.
  C_9 - Symmetrical lens: They are the intersection of two congruent circular disks. The extremal compact convex sets are the point and the disk.
  C_{10} - Symmetrical disks with two peaks: They are the convex hulls of a disk and two symmetrically placed points. The disk radius value varies between 0 and the half of the line segment length. The extremal compact convex sets are the line segment and the disk, respectively.
  C_{11} - Diamonds: The ratio between the top angles varies in $[0, 1]$. When it reaches the lower and upper bounds, the diamond becomes a line segment and a square, respectively.
  C_{12} - Rectangles terminated by equilateral triangles: The ratio between the width and the length of the rectangle varies in $[0, 1]$. Equilateral triangles are placed on two opposite edges. When the ratio reaches the lower and upper bounds, the resulting compact convex set becomes a line segment and a "1/2" diamond, respectively.
  C_{13} - Rectangles terminated by isosceles rectangle triangles: The ratio between the width and the length of the rectangle varies in $[0, 1]$. Isosceles rectangle triangles are placed on two opposite edges. When the ratio reaches the lower and upper bounds, the resulting compact convex set becomes a line segment and a square, respectively.

- Family $\mathcal{F}^c_{2.3}$:
  C_{14} - Yamanouti triangles [27]: The radius value varies between the height and the edge length of an equilateral triangle. The extremal compact convex sets are the equilateral triangle and the Reuleaux triangle, respectively.
  C_{15} - Disk-equilateral triangle intersections: They are the intersections of an equilateral triangle and a disk centered on the center of mass with a radius varying between the radii of inscribed and circumscribed circles. The extremal compact convex sets are the disk and the equilateral triangle, respectively.
  C_{16} - Dilated (disk) equilateral triangles: They are obtained by the dilation of an equilateral triangle with a disk of radius included in $[0, +\infty[$. When the radius value reaches the lower bound, the resulting compact convex set becomes an equilateral triangle. When the radius tends to infinity, the resulting compact convex set tends to the disk.
  C_{17} - Regular odd polygons: They are regular polygons with a positive odd edge number. In the shape diagrams, the real positions of these compact convex sets do not describe a curve because it is not continuous (the edge number is necessarily an integer) but they are along a curve. Theorically, the extremal compact convex sets are the point and the disk. In the following shape diagrams, only the curve from the equilateral triangle to the disk is drawn.
  C_{18} - Reuleaux odd polygons: They are Reuleaux polygons with a positive odd edge number. In the shape diagrams, the real positions of these compact convex sets do not describe a curve because it is not continuous (the edge number is necessarily an integer) but they are along a curve. Theorically, the extremal compact convex sets are the point and the disk. In the following shape diagrams, only the curve from the Reuleaux triangle to the disk is drawn.
- Family $\mathcal{F}^c_{2.4}$:
  C_{19} - "Yamanouti" squares: They are defined in a similar way as the Yamanouti triangles, but from the middle of the opposite edges. The extremal compact convex sets are the square and the "Reuleaux" square.
  C_{20} - Disk-square intersections: They are the intersections of a square and a disk centered on the center of mass with a radius varying between the radii of inscribed and circumscribed circles. The extremal compact convex sets are the disk and the square, respectively.
  C_{21} - Dilated (disk) squares: They are obtained by the dilation of a square with a disk of radius included in $[0, +\infty[$. When the radius value reaches the lower bound, the resulting compact convex set becomes a square. When the radius tends to infinity, the resulting compact convex set tends to the disk.
  C_{22} - Regular even polygons: They are regular polygons with a positive even edge number. In the shape diagrams, the real positions of these compact convex sets do not describe a curve because it is not continuous (the edge number is necessarily an integer) but they are along a curve. Theorically, the extremal compact convex sets are the line segment and the disk. In the following shape diagrams, only the curve from the square to the disk is drawn.
  C_{23} - "Reuleaux" even polygons: They are defined in a similar way as the Reuleaux odd polygons, but from the middle of the opposite edges. In the

shape diagrams, the real positions of these compact convex sets do not describe a curve because it is not continuous (the edge number is necessarily an integer) but they are along a curve. Theorically, the extremal compact convex sets are the line segment and the disk. In the following shape diagrams, only the curve from the "Reuleaux" square to the disk is drawn.

For the compact convex sets of each class, the morphometrical functionals are computed. In each shape diagram $\mathcal{D}_k$, $k \in [\![1, 31]\!]$, a compact convex set class $i \in [\![1, 23]\!]$ is represented by a parametric curve $\mathcal{C}_{i,k}(t)$ since the class is infinite and bounded by the two extremal sets. For the considered compact convex set classes, the extremal compact convex set are in the family $\mathcal{F}_1^c$ (Figure 2.3). For example, up to a similitude transformation, an infinite class of rectangles exists, from the line segment to the square.

Figures 5.5, 5.6, 5.7 and 5.8 illustrate some of these shape diagrams, chosen according to the results synthetized in section 6.

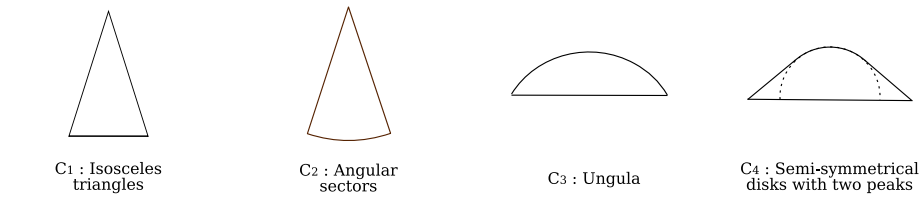

Figure 5.1: Family $\mathcal{F}_{2.1}^{c}$ of 2D analytic compact convex sets with one degree of freedom and one symmetrical axis.

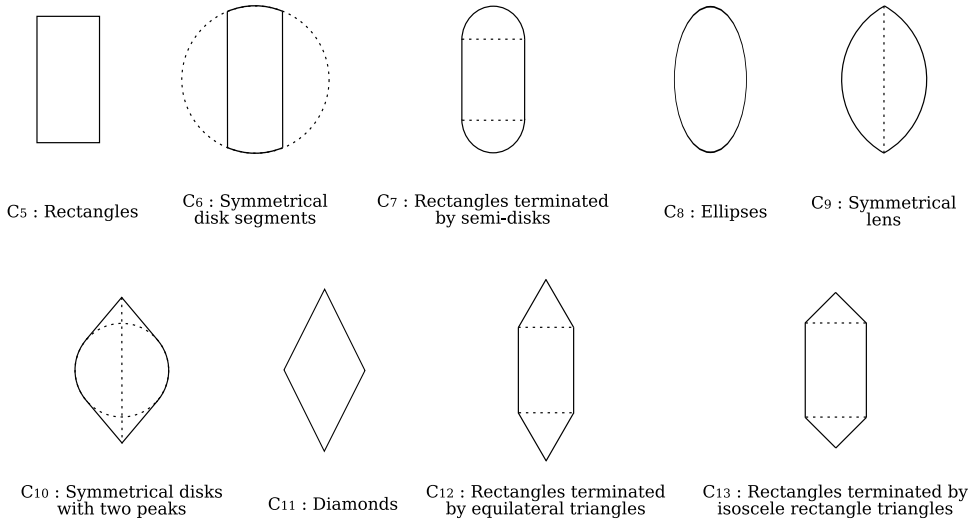

Figure 5.2: Family $\mathcal{F}_{2.2}^{c}$ of 2D analytic compact convex sets with one degree of freedom and two symmetrical axes.

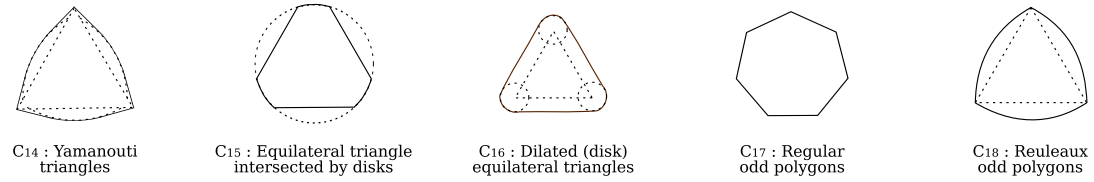

Figure 5.3: Family $\mathcal{F}_{2.3}^{c}$ of 2D analytic compact convex sets with one degree of freedom and an odd number (strictly greater to 1) of symmetrical axes.

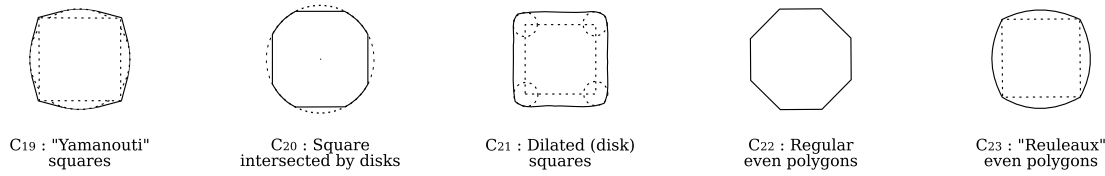

Figure 5.4: Family $\mathcal{F}_{2.4}^{c}$ of 2D analytic compact convex sets with one degree of freedom and an even number (strictly greater to 2) of symmetrical axes.

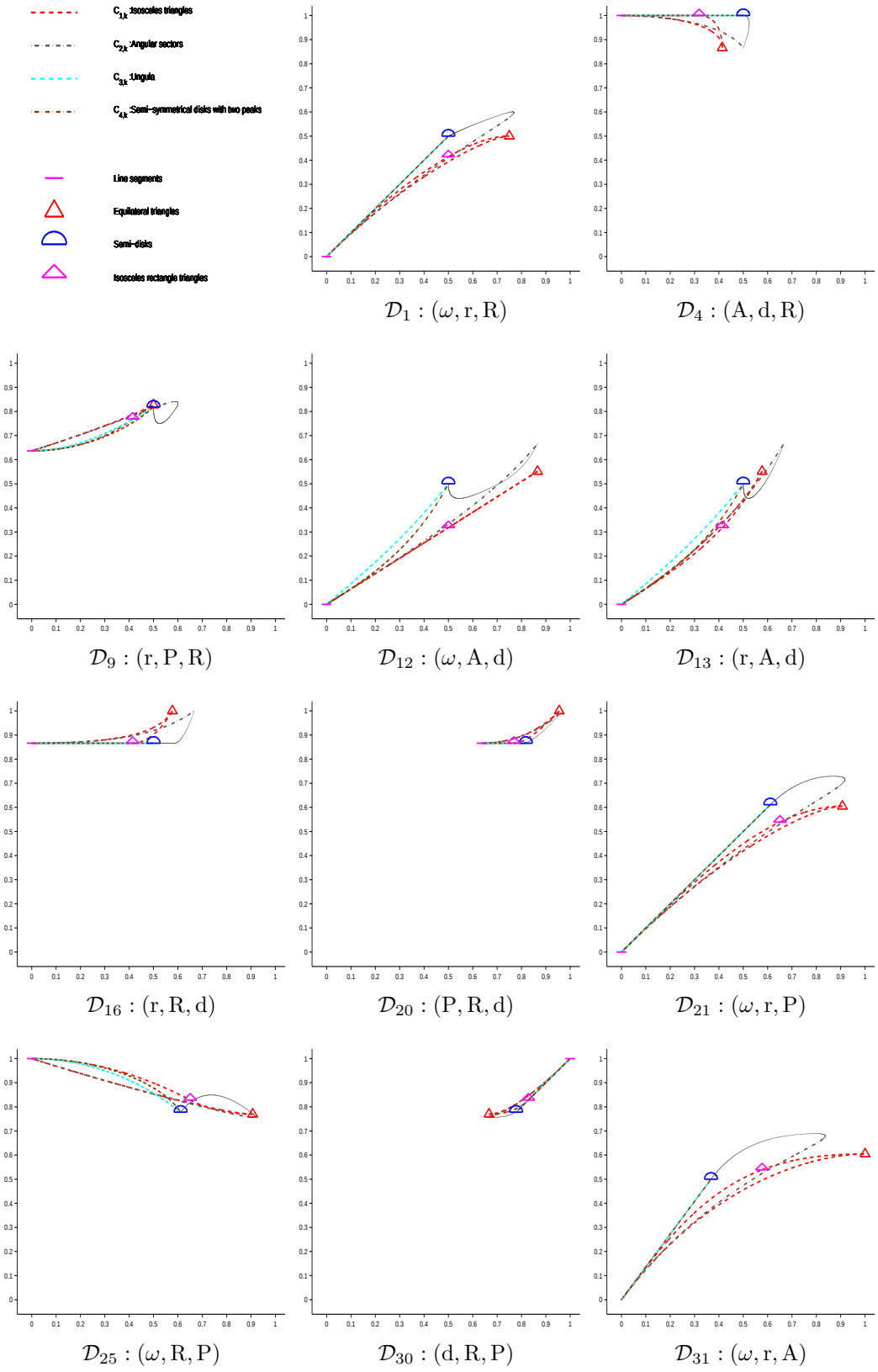

Figure 5.5: Family $\mathcal{F}^c_{2.1}$ of analytic compact convex sets with one degree of freedom and one symmetrical axis mapped into eleven shape diagrams (chosen according to the results synthetized in section 6).

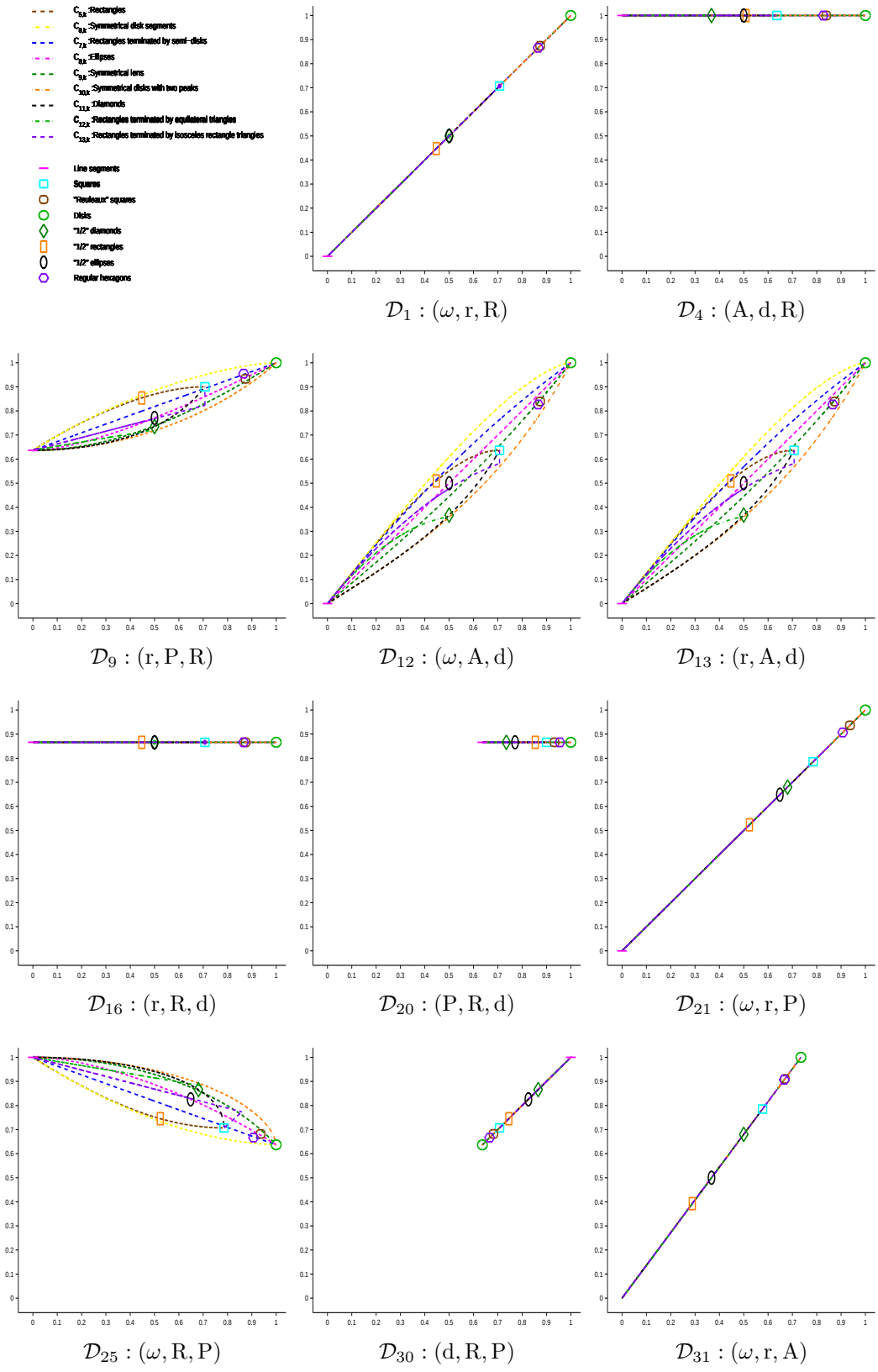

Figure 5.6: Family $\mathcal{F}^c_{2,2}$ of analytic compact convex sets with one degree of freedom and two symmetrical axes mapped into eleven shape diagrams (chosen according to the results synthetized in section 6).

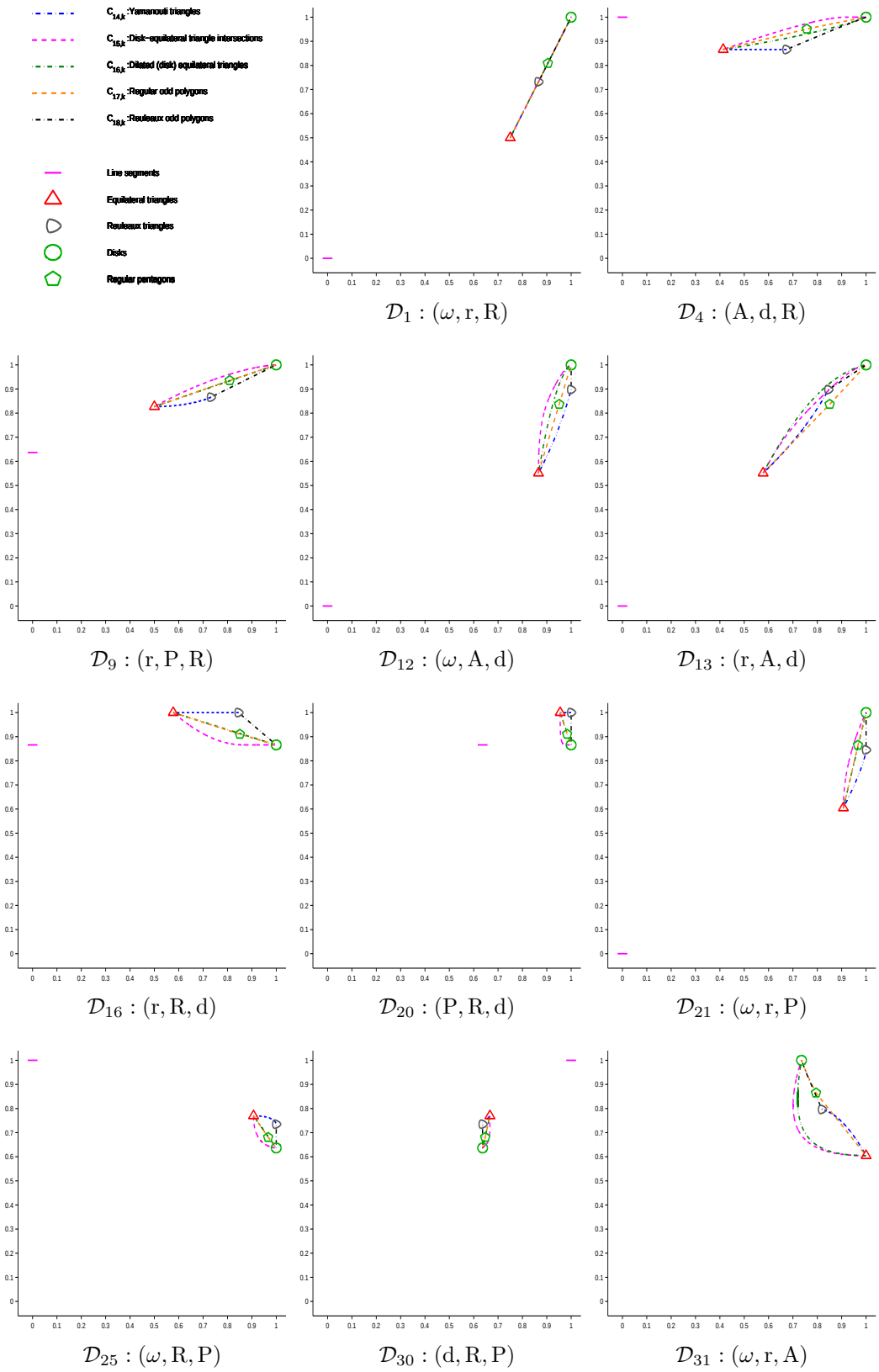

Figure 5.7: Family $\mathcal{F}^c_{2.3}$ of analytic compact convex sets with one degree of freedom and an odd number strictly greater to 1 of symmetrical axes mapped into eleven shape diagrams (chosen according to the results synthetized in section 6).

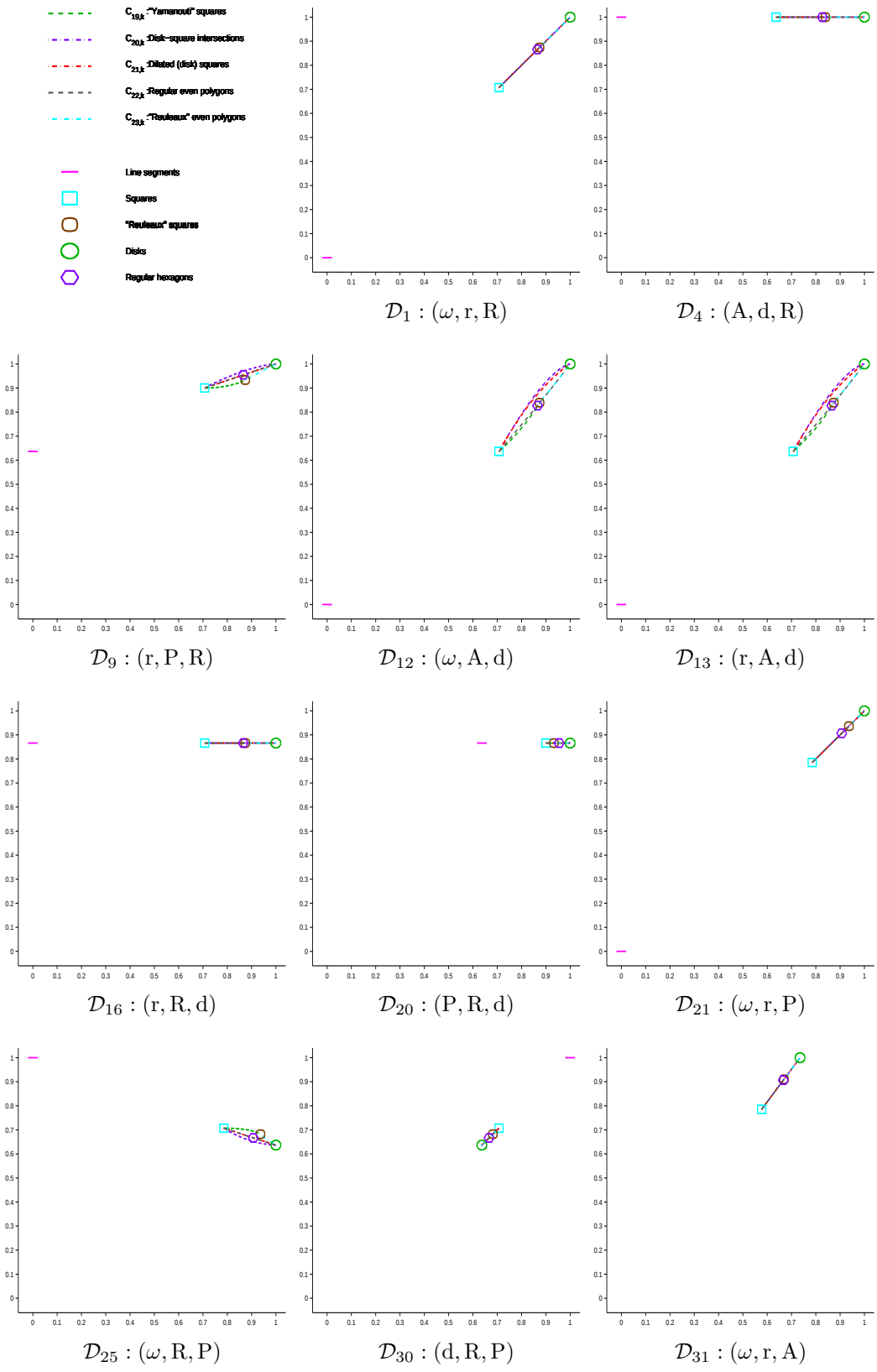

Figure 5.8: Family $\mathcal{F}^c_{2.4}$ of analytic compact convex sets with one degree of freedom and an even number strictly greater to 2 of symmetrical axes mapped into eleven shape diagrams (chosen according to the results synthetized in section 6).

5.2 Overlapping quantification An overlapping of curves is visible in some shape diagrams. Its quantification is based on a discretization of the spatial domain $[0,1]^2$ of the shape diagrams. Let $n \in \mathbb{N}^*$, the discretization of a curve $\mathcal{C}_{i,k}$, $i \in [\![1,23]\!]$, $k \in [\![1,31]\!]$, is denoted $C_{i,k} : [\![0,n]\!]^2 \to \{0,1\}$ and defined as following, $\forall (x,y) \in [\![0,n]\!]^2$:

$$C_{i,k}(x,y) = \begin{cases} 1 & \text{if } \exists t_0 \in \mathbb{R} \mid \left(x-\frac{1}{2}\right)\frac{1}{n} \leq \mathcal{C}_{i,k}(t_0)\ \vec{u} \leq \left(x+\frac{1}{2}\right)\frac{1}{n} \\ & \qquad\qquad \left(y-\frac{1}{2}\right)\frac{1}{n} \leq \mathcal{C}_{i,k}(t_0)\ \vec{v} \leq \left(y+\frac{1}{2}\right)\frac{1}{n} \\ 0 & \text{elsewhere} \end{cases}$$

where $\vec{u}$ and $\vec{v}$ are the unit vectors along the abscissa and ordinate axes, respectively.

When all curves of a shape diagram are considered, two discretized shape diagrams are built (Figure 5.9):

- the "binary" discretized shape diagram, indicating where the curves are located (Figure 5.9.(a)).
  It is denoted $D_k^{max} : [\![0,n]\!]^2 \to \{0,1\}$ and defined $\forall (x,y) \in [\![0,n]\!]^2$ by:
  $$D_k^{max}(x,y) = \max_{i \in [\![1,23]\!]} C_{i,k}(x,y)$$
- the "intensity" discretized shape diagram, indicating the intensities of curves overlapping, i.e. the counts of curve overlaps (Figure 5.9.(b)).
  It is denoted $D_k^{sum} : [\![0,n]\!]^2 \to \mathbb{N}$ and defined $\forall (x,y) \in [\![0,n]\!]^2$ by:
  $$D_k^{sum}(x,y) = \sum_{i \in [\![1,23]\!]} C_{i,k}(x,y)$$

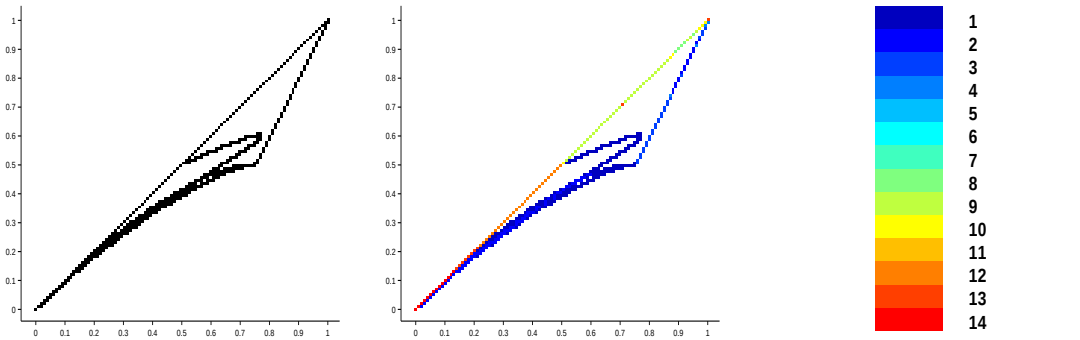

(a) D_1^{max} (b) D_1^{sum} Overlapping intensities

Figure 5.9: "Intensity" discretized shape diagram $D_1 : (\omega, \mathrm{r}, \mathrm{R})$ ($n = 100$) with the twenty-three curves representing the compact convex set classes with one degree of freedom.

Finally, Equation 5.1 quantifies (by a measurement ranging between 0 and 1) the overlapping of all curves for each shape diagram $\mathcal{D}_k$, $k \in [\![1,31]\!]$. A high (resp. low) value for this ratio means a strong (resp. weak) overlapping. This quantification depends on the discretization level n. Thus, when the computation is done for various n values, not only the curves overlapping is considered but also the curves

proximity (small n value).

$$\text{Overlapping}_n(\mathcal{D}_k) = 1 - \frac{\sum_{(x,y)\in[\![0,n]\!]^2} D_k^{max}(x,y)}{\sum_{(x,y)\in[\![0,n]\!]^2} D_k^{sum}(x,y)} \tag{5.1}$$

Figure 6.1 illustrates the discretized shape diagrams ($n = 100$) with overlapping intensities, and Figure 6.2 shows the quantification of curves overlapping (representing the compact convex set classes) for some shape diagrams, according to the n values 100 and 1000.

Several informations can be extracted from these graphs:

- The graphs representing the 2D analytic compact convex set classes of the families $\mathcal{F}_{2.2}^c$ and $\mathcal{F}_{2.4}^c$ show a strong overlap (from $n = 1000$) for the shape diagrams $\mathcal{D}_1$, $\mathcal{D}_4$, $\mathcal{D}_5$, $\mathcal{D}_6$, $\mathcal{D}_{10}$, $\mathcal{D}_{11}$, $\mathcal{D}_{14}$, $\mathcal{D}_{15}$, $\mathcal{D}_{16}$, $\mathcal{D}_{20}$, $\mathcal{D}_{21}$, $\mathcal{D}_{30}$ and $\mathcal{D}_{31}$.
- The graphs representing the 2D analytic compact convex set classes of the family $\mathcal{F}_{2.3}^c$ show a strong overlap (from $n = 1000$) for the shape diagram $\mathcal{D}_1$. They are close to each other (strong overlap from $n = 100$) in the shape diagrams $\mathcal{D}_{17}$, $\mathcal{D}_{18}$, $\mathcal{D}_{19}$, $\mathcal{D}_{27}$, $\mathcal{D}_{28}$ and $\mathcal{D}_{29}$.

6 Synthesis

To obtain a strong discrimination of 2D analytic compact convex sets, it is necessary to have both a strong dispersion and a weak overlapping.

- The shape diagrams $\mathcal{D}_{10}$, $\mathcal{D}_{20}$ and $\mathcal{D}_{30}$ are excluded due to their weak dispersion and overlapping results, whatever the considered compact convex sets.
- In the shape diagrams $\mathcal{D}_4$, $\mathcal{D}_5$, $\mathcal{D}_6$, $\mathcal{D}_{14}$, $\mathcal{D}_{15}$ and $\mathcal{D}_{16}$, only the family $\mathcal{F}_{2.3}^c$ shows a weak overlapping. Futhermore, their dispersion quantification is moderate and even somewhat below.
- In the shape diagram $\mathcal{D}_{31}$, the families of $\mathcal{F}_{2.1}^c$ and $\mathcal{F}_{2.3}^c$ show a weak overlapping. Futhermore, its dispersion quantification is moderate.
- In the shape diagrams $\mathcal{D}_7$, $\mathcal{D}_8$, $\mathcal{D}_9$, $\mathcal{D}_{17}$, $\mathcal{D}_{18}$, $\mathcal{D}_{19}$, $\mathcal{D}_{24}$, $\mathcal{D}_{25}$, $\mathcal{D}_{26}$, $\mathcal{D}_{27}$, $\mathcal{D}_{28}$ and $\mathcal{D}_{29}$, all the families considered in this paper show a weak overlapping. But in $\mathcal{D}_{17}$, $\mathcal{D}_{18}$, $\mathcal{D}_{19}$, $\mathcal{D}_{27}$, $\mathcal{D}_{28}$ and $\mathcal{D}_{29}$, the compact convex set classes of $\mathcal{F}_{2.3}^c$ are located close together. However, the dispersion quantification of all these shape diagrams are moderate.
- The dispersion quantification of the shape diagrams $\mathcal{D}_1$, $\mathcal{D}_2$, $\mathcal{D}_3$, $\mathcal{D}_{11}$, $\mathcal{D}_{12}$, $\mathcal{D}_{13}$, $\mathcal{D}_{21}$, $\mathcal{D}_{22}$ and $\mathcal{D}_{23}$ gives strong values, particularly for $\mathcal{D}_{22}$. In the shape diagram $\mathcal{D}_1$, only the family $\mathcal{F}_{2.1}^c$ shows a weak overlapping, and in the shape diagrams $\mathcal{D}_{11}$ and $\mathcal{D}_{21}$, only the families of $\mathcal{F}_{2.1}^c$ and $\mathcal{F}_{2.3}^c$ show a weak overlapping. It remains the shape diagrams $\mathcal{D}_2$, $\mathcal{D}_3$, $\mathcal{D}_{12}$, $\mathcal{D}_{13}$, $\mathcal{D}_{22}$, $\mathcal{D}_{23}$ that, in addition to their strong dispersion, provide a weak overlapping of the compact convex set classes considered in this paper.

Futhermore, among the shape diagrams $\mathcal{D}_2$, $\mathcal{D}_3$, $\mathcal{D}_{12}$, $\mathcal{D}_{13}$, $\mathcal{D}_{22}$ and $\mathcal{D}_{23}$ that obtain the best results for dispersion and overlapping quantifications, only $\mathcal{D}_3$, $\mathcal{D}_{12}$, $\mathcal{D}_{22}$ and $\mathcal{D}_{23}$ are based on known complete systems of inequalities. Observing in details the representation of quantifications for these four shape diagrams, $\mathcal{D}_{12}$ is retained for shape discrimination of analytic compact convex sets.

This analysis is summarized in Table 6.1.

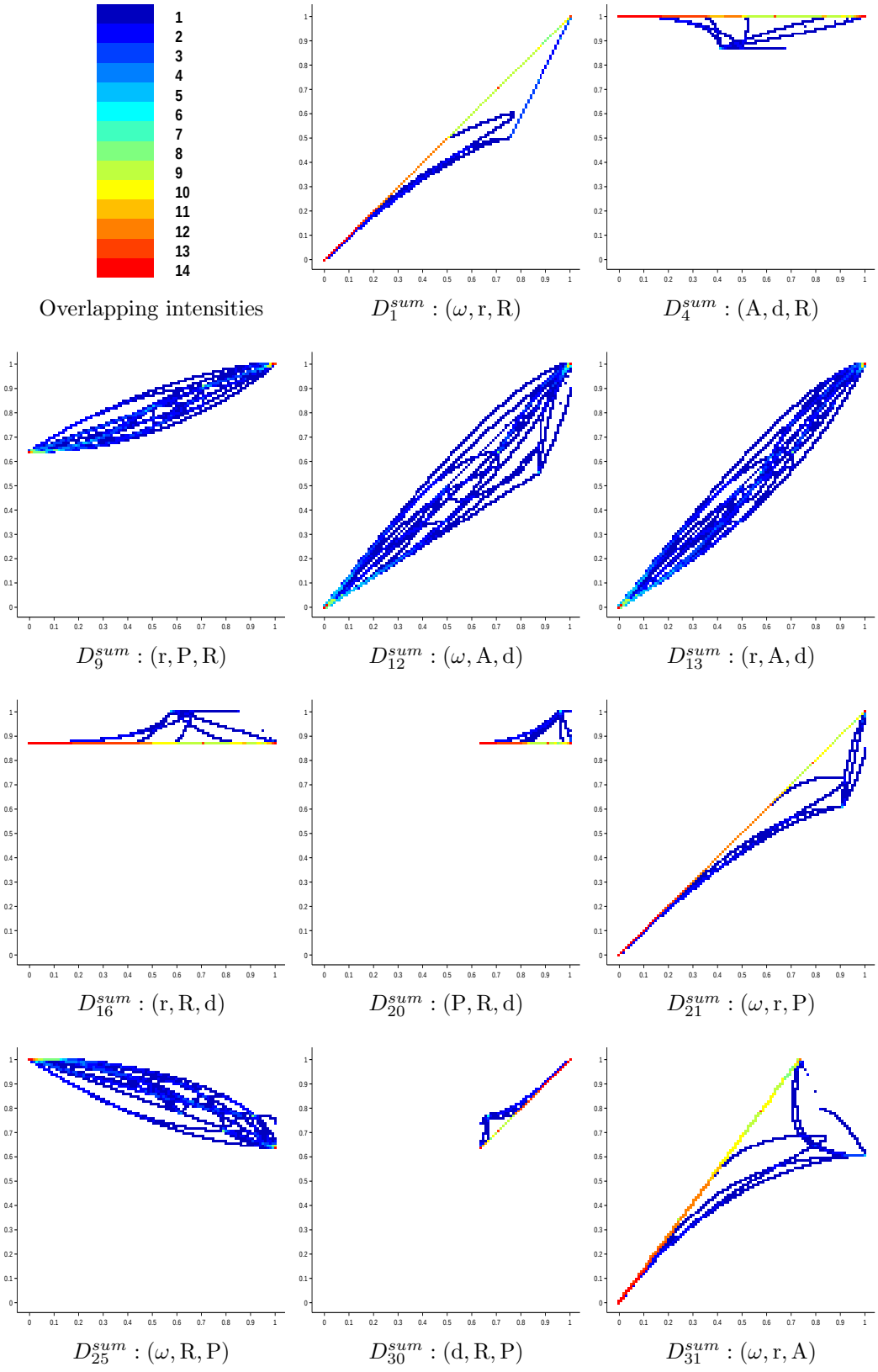

Figure 6.1: "Intensity" discretized shape diagram D_k^{sum} ($n = 100$) with the twenty-three curves representing the compact convex set classes with one degree of freedom.

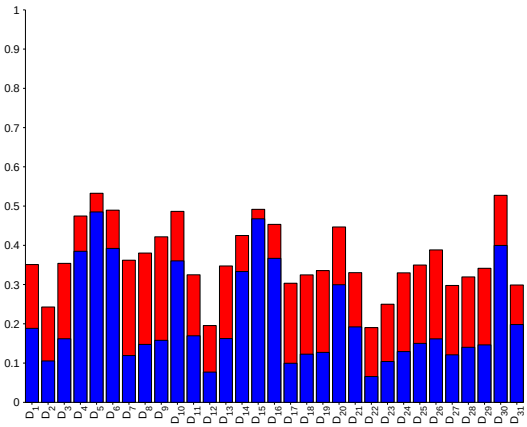

Overlapping quantification for the family $\mathcal{F}_{2.1}^{c}$ of compact convex sets with one degree of freedom and one symmetrical axis.

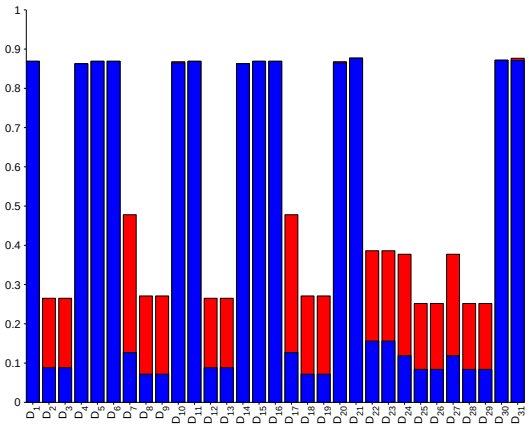

Overlapping quantification for the family $\mathcal{F}_{2.2}^{c}$ of compact convex sets with one degree of freedom and two symmetrical axes.

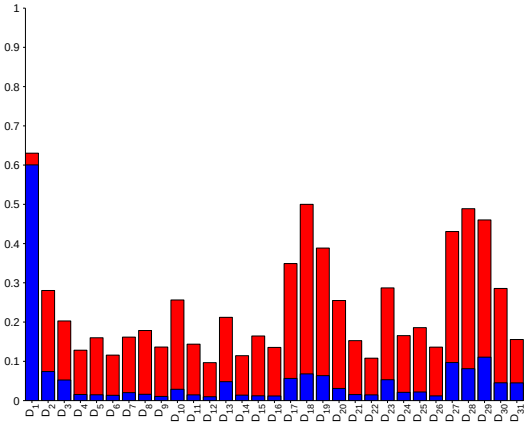

Overlapping quantification for the family $\mathcal{F}_{2.3}^{c}$ of compact convex sets with one degree of freedom and an odd number strictly greater to 1 of symmetrical axes.

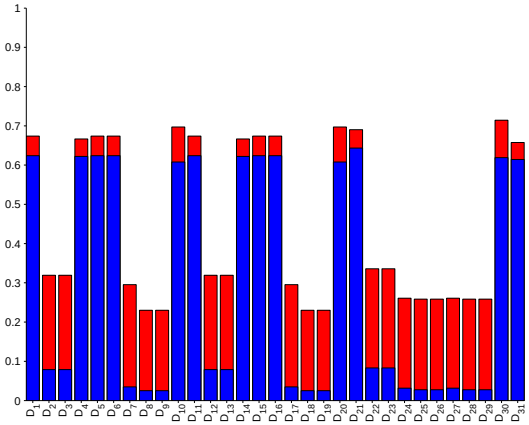

Overlapping quantification for the family $\mathcal{F}_{2.4}^{c}$ of compact convex sets with one degree of freedom and an even number strictly greater to 2 of symmetrical axes.

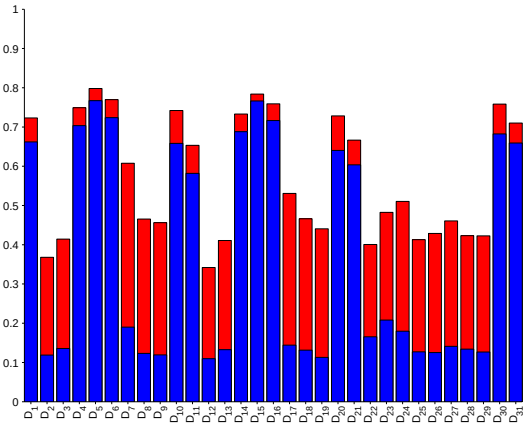

Overlapping quantification for the twenty-three classes of compact convex sets with one degree of freedom.

Figure 6.2: Overlapping quantification for the thirty-one shape diagrams $\mathcal{D}_k$, $k \in [\![1, 31]\!]$, with $n = 100$ in red, and $n = 1000$ in blue.

	Complete system of inequalities	Non-complete system of inequalities
Strong discrimination	$\mathcal{D}_3$, $\boxed{\mathcal{D}_{12}}$, $\mathcal{D}_{22}$, $\mathcal{D}_{23}$	$\mathcal{D}_2$, $\boxed{\mathcal{D}_{13}}$
Moderate discrimination	$\boxed{\mathcal{D}_1}$, $\mathcal{D}_7$, $\boxed{\mathcal{D}_9}$, $\mathcal{D}_{11}$, $\mathcal{D}_{18}$, $\mathcal{D}_{24}$, $\mathcal{D}_{26}$, $\mathcal{D}_{28}$	$\mathcal{D}_8$, $\mathcal{D}_{17}$, $\mathcal{D}_{19}$, $\boxed{\mathcal{D}_{21}}$, $\boxed{\mathcal{D}_{25}}$, $\mathcal{D}_{27}$, $\mathcal{D}_{29}$
Weak discrimination	$\boxed{\mathcal{D}_4}$, $\mathcal{D}_5$, $\mathcal{D}_6$, $\mathcal{D}_{10}$, $\mathcal{D}_{14}$, $\mathcal{D}_{15}$, $\boxed{\mathcal{D}_{16}}$, $\boxed{\mathcal{D}_{20}}$, $\boxed{\mathcal{D}_{30}}$	$\boxed{\mathcal{D}_{31}}$

Table 6.1: Shape diagrams classification according to their quality of shape discrimination of analytic compact convex sets and according to the completeness of associated systems of inequalities.

In this paper, only some shape diagrams have been illustrated. The choice was based on the results of shape discrimination (dispersion and overlapping studies) and on the results of similarities between shape diagrams (subsection 4.2). The aim was to illustrate dissimilar shape diagrams with different qualities of shape discrimination, and shape diagrams with different completeness of associated systems of inequalities. The framed shape diagrams of Table 6.1 are those illustrated throughout this paper.

7 Conclusion

This paper has dealed with shape diagrams of 2D non-empty analytic compact convex sets built from six geometrical functionals: the area, the perimeter, the radii of the inscribed and circumscribed circles, and the minimum and maximum Feret diameters. Each such a set is represented by a point within a shape diagram whose coordinates are morphometrical functionals defined as normalized ratios of geometrical functionals. From existing morphometrical functionals for these sets, thirty-one shape diagrams can be built. A detailed comparative study has been performed in order to analyze the representation relevance and discrimination power of these shape diagrams. It is based on the dispersion and overlapping quantifications from compact convex set locations in diagrams. Among all the shape diagrams, six present a strong shape discrimination of sets, four are based on complete system of inequalities. Among these four diagrams, the shape diagram $\mathcal{D}_{12} : (\omega, \mathrm{A}, \mathrm{d})$ is retained for its representation relevance and discrimination power.

This paper reports the first part of a general comparative study of shape diagrams. The focus was placed on analytic compact convex sets. However, most of these shape diagrams can also been applied to more general compact sets than compact convex sets. The second and third parts of the comparative study are published

in two following papers [19, 20]. They are focused on analytic simply connected compact sets and convexity discrimination for analytic and discretized simply connected compact sets, respectively.

8 Acknowledgments

The authors would like to thank M.A. Hernández Cifre for her constructive comments.

References

[1] W. Blaschke. Konvexe Bereiche gegebener konstanter Breite und kleinsten Inhalts. *Mathematische Annalen.* **76**: 504-513 (1915).

[2] W. Blaschke. Eine frage über konvexe körper. *Jahresbericht Deutsch. Math.-Verein.* **25**: 121-125 (1916).

[3] J.D. Boissonnat and M. Yvinec. *Algorithmic geometry.* Cambridge University Press (1998).

[4] T. Bonnesen and W. Fenchel. *Theorie der konvexen körper.* Springer-Verlag, Berlin (1934, 1974); Chelsea, New-York (1948).

[5] K. Böröczky Jr., M.A. Hernández Cifre and G. Salinas. Optimizing area and perimeter of convex sets for fixed circumradius and inradius. *Monatshefte für Mathematik.* **138**: 95-110 (2003).

[6] E. Diday. Croisements, ordres et ultramétriques. *Mathématiques et Sciences humaines.* **83**: 31-54 (1983).

[7] H.G. Eggleston. A proof of Blaschke's theorem on the Reuleaux triangle. *Quarterly Journal of Mathematics, Oxford* **3(2)**: 296-297 (1952).

[8] L.R. Feret. La grosseur des grains des matières pulvérulentes. *Premières Communications de la Nouvelle Association Internationale pour l'Essai des Matériaux. Groupe D*: 428-436 Zürich (1930).

[9] M.A. Hernández Cifre. Is there a planar convex set with given width, diameter, and inradius ? *American Mathematical Monthly.* **107**: 893-900 (2000).

[10] M.A. Hernández Cifre and S. Segura Gomis. The missing boundaries of the Santaló diagrams for the cases (d,ω,R) and (ω,R,r). *Discrete and Computational Geometry.* **23**: 381-388 (2000).

[11] M.A. Hernández Cifre, G. Salinas and S. Segura Gomis. Complete Systems of Inequalities. *Journal of Inequalities in Pure and Applied Mathematics.* **2(1-10)**: 1-12 (2001).

[12] M.A. Hernández Cifre. Optimizing the perimeter and the area of convex sets with fixed diameter and circumradius. *Archiv der Mathematik.* **79**: 147-157 (2002).

[13] P.W. Hillock and P.R. Scott. Inequalities for lattice constrained planar convex sets. *Journal of Inequalities in Pure and Applied Mathematics.* **3(2-23)**: 1-10 (2002).

[14] R. Osserman. The isoperimetric inequality. *Bulletin of the American Mathematical Society* **84**: 1182-1238 (1978).

[15] R. Osserman. Bonnesen style isoperimetric inequalities. *American Mathematical Monthly.* **86**: 1-29 (1979).

[16] B.N. Raby, M. Polette, C. Gilles, C. Clavel, K. Strumane, M. Matos, J.M. Zahm, F. Van Roy, N. Bonnet and P. Birembaut. Quantitative cell dispersion analysis: new test to measure tumor cell aggressiveness. *International Union Against Cancer.* **93**: 644-652 (2001).

[17] S. Ramanujan. *Ramanujan's Collected Works*, Chelsea, New York (1962).

[18] F. Reuleaux. *The Kinematics of Machinery: Outlines of a Theory of Machines.* German original (1875). Translated by A. Kennedy, MacMillan and Co., London (1876). Reprinted by Dover, New-York (1963).

[19] S. Rivollier, J. Debayle and J.C. Pinoli. Shape diagrams for 2D compact sets - Part II: analytic simply connected sets. *Australian Journal of Mathematical Analysis and Applications.* **7(2-4)**: 1-21 (2010).

[20] S. Rivollier, J. Debayle and J.C. Pinoli. Shape diagrams for 2D compact sets - Part III: convexity discrimination for analytic and discretized simply connected sets. *Australian Journal of Mathematical Analysis and Applications.* **7(2-5)**: 1-18 (2010).

[21] L.A. Santaló. Sobre los sistemas completos de desigualdades entre tres elementos de una figura convexa plana. *Math. Notae.* **17**: 82-104 (1961).

[22] P.R. Scott. A family of inequalities for convex sets. *Bulletin of the Australian Mathematical Society* **20**: 237-245 (1979).

[23] P.R. Scott and P.W. Awyong. Inequalities for convex sets. *Journal of Inequalities in Pure and Applied Mathematics.* **1(1-6)**: 1-6 (2000).

[24] A. Siegel. An isoperimetric theorem in plane geometry. *Discrete and Computational Geometry.* **29(2)**: 239-255 (2003).

[25] M.B. Villarino. A note on the accuracy of Ramanujan's approximative formula for the perimeter of an ellipse. *Journal of Inequalities in Pure and Applied Mathematics.* **7(1-21)**: 1-10 (2006).

[26] I.M. Yaglom and V.G. Boltanskii. *Convex figures,* translated by P.J. Kelly and L.F. Walton, Holt, Rinehart and Winton (1961).

[27] M. Yamanouti. Notes on closed convex sets. *Proceedings of the Physico-Mathematical Society of Japan Ser.* **14**: 605-609 (1932).

Ecole Nationale Supérieure des Mines de Saint-Etienne, CIS - LPMG, UMR CNRS 5148, 158 cours Fauriel, 42023 Saint-Etienne cedex 2, France, Tel.: +33-477-420219 / Fax: +33-477-499694,

E-mail address: rivollier@emse.fr ; debayle@emse.fr ; pinoli@emse.fr